AN INVESTIGATION OF VORTEX SHEDDING AS RELATED TO THE SELF-EXCITED TORSIONAL OSCILLATION OF AN AIRFOIL

Thesis by

Raymond L. Chuan

In Partial Fulfillment of the Requirements

for the Degree of Aeronautical Engineer

California Institute of Technology

Pasadena, California

June, 1948

ACKNOWLEDGEMENT

The author wishes to express his appreciation to Professor L. G. Dunn and Mr. Henry T. Nagamatsu under whose guidance this research was performed, and to members of the Laboratory staff for their assistance in carrying out this research program.

TABLE OF CONTENTS

I. SUMMARY

This report covers the results of the experimental investigation of the self-excited torsional oscillation of a NACA 0006 airfoil suspended elastically. The relationship between the torsional oscillation and the shedding of vortices was investigated for this airfoil.

Two types of oscillation phenomena were found in the investigation. One type, exhibited by cases with angles of attack just above stall, persisted with increasing velocity without reaching any apparent limit within the range of velocity attainable in the present windtunnel. The other type, exhibited by cases with higher angles of attack, only showed self-excited oscillations in a certain range of velocity, the range decreasing with increasing angle of attack.

II. INTRODUCTION

The investigation of the failure of the Tacoma Narrows Bridge in 1941 indicated that a flat plate exposed at moderate angle of attack to a windstream exhibited self-excited torsional oscillations of considerable amplitude. The National Advisory Committee for Aeronautics subsequently sponsored a program at the Guggenheim Aeronautical Laboratory, California Institute of Technology to further study this phenomenon.

Reference 1 covered test results of bending oscillations and preliminary work on torsional oscillations. Reference 2 dealt with torsional oscillations only and indicated that additional research was necessary to investigate the mechanism for the starting of the self-excited torsional oscillations as related to the shedding of vortices. Reference 2 indicated that there was no upper limit to the range of velocities in which the oscillations occurred. The present investigation showed that for angles of attack beyond a certain limit there were upper limits to the velocities at which self-excited oscillations occurred. The results of Reference 2 indicated that the amplitude of the oscillations depended on past history. Therefore, in the present research program the airfoil was allowed to start from rest every time the velocity was varied. The study of the vortex shedding in an attempt to relate it to the oscillation was accomplished by the use of hot-wire anemometers.

III. SYMBOLS

α	geometric angle of attack of airfoil when stationary, in degrees
V	wind velocity, in feet per second
V_1	lower critical velocity at which oscillation starts
V_2	upper critical velocity at which oscillation no longer starts
V_3	velocity at which maximum amplitude occurs
θ	amplitude of oscillation in degrees
$\theta_{max.}$	maximum amplitude of oscillation at a given angle of attack
n	frequency of oscillation
N	frequency of vortex shedding with stationary airfoil
N_1	N corresponding to V_1
N_2	N corresponding to V_2
N_3	N corresponding to V_3
b	airfoil chord
K	dimensionless Karman number
ΔH	difference in total head between free stream and in the wake

IV. DESCRIPTION OF APPARATUS

An open-return windtunnel, as shown schematically in Figure 1, and described in Reference 1, was used for this research program. To insure that oscillations were not caused by any fluctuation in the flow through the test section, three screens were placed at the entry of the contraction section. Two of these were made of cheese-cloth, and the third was made of 20-mesh copper screen. They were spaced at one foot intervals. A $1\frac{1}{2}$ inch gap was left between the diffuser section and the fan section to prevent any oscillation of the engine-propeller section from being transmitted to the working section.

The power was supplied by a conventional automobile engine with a maximum output of 125 h.p. and driving an eight-blade propeller through a transmission system permitting three gear ratios. The engine was mounted outside the building, so a remote control system was necessary to vary the speed. This was accomplished by actuating the engine throttle valve by a lead-screw driven by a reversible d.c. motor. Velocity variation as low as $\frac{1}{2}$ f.p.s. could be achieved by this method.

The suspension system consisted of a 24 ST dural rod mounted on each end of the airfoil as shown in Figure 2. This allowed maximum freedom for torsional oscillation while affording little freedom for any other mode of motion. The linear relation of stress and strain of these torsion rods furnished a convenient means of measuring both the frequency and amplitude of the oscillations by the use of a strain-gage. Two sets of rods were used in this experiment. With the suspended mass constant, the frequency of oscillation of the airfoil

depends on the diameter of the rods. One set of dural rods (designated Suspension #1) of 0.188 inch diameter was used to obtain a torsional frequency of approximately 12 cycles per second and another set (designated Suspension #2) of 0.25 inch diameter had a frequency of approximately 20 c.p.s.

The NACA 0006 airfoil was of laminated wood construction with a 9-inch chord and 41-inch span. Each end of the airfoil was fitted with two dural blocks into which fitted the pins that connected the airfoil to the suspension system. The details of the suspension system are shown in Figure 2.

The amplitude of the oscillation was measured by means of a strain-gage mounted on one of the suspension rods at 45° to the axis of the rod. Thus, the deflection of the strain-gage was directly proportional to the angle of twist. The output of the strain-gage was fed through a 6-channel amplifier designed for both strain-gage and hot-wire measurements. The current through a strain-gage, supplied by a 12-volt d.c. source, was approximately 10 milliamperes. The method of calibration used here was such that the fluctuation in the voltage across the strain-gage or in the gain of the amplifier could not affect the measurement of the angular deflections. This was accomplished by shunting the strain-gage with any one of several precision resistors. With a resistor shunted across the undeflected strain-gage, the reduced net resistance was measured with a Wheatstone Bridge. Then, the shunt was removed and the airfoil was deflected to such a position as to give the same amount of reduction in the resistance. The angular deflection at this point was recorded. This was done with four different shunting resistors. By means of a selector switch and

a micro switch any one of these four shunts could be placed across the strain-gage, each shunt corresponding to a known angular deflection. The output of the amplifier was fed into a 6-channel recording oscillograph, Heiland Type A-400R6. The calibration appeared as a stepped trace on the recording paper. By comparing the height of the step and the subsequent oscillation record, the exact angular deflection could be obtained independent of any variation in the voltage across the strain-gage or in the amplifier gain. The oscillograph had a timer which marked 0.01 second timing lines on the recording tape.

Two sets of hot-wire anemometers were used to measure the vortex shedding frequency. One set was mounted fixed with respect to the tunnel, while the other was mounted on the airfoil itself and moved with it. The fixed hot-wires were mounted on streamlined dural struts, one protruding into the windstream from the bottom of the test section and the other from the top. Both struts were mounted on traversing mechanisms permitting motions both vertically and along the windstream direction. The moving hot-wires were mounted by means of rigid frames made of 1/8 inch copper tubing secured to the top surface of the airfoil. One such hot-wire was mounted near the leading edge and the other one near the trailing edge, as shown in Figure 2a. The anemometers were made of $\frac{1}{4}$ mil. platinum wire with length of approximately 3/16 inch, as shown in Figure 2a. Approximately 100 to 150 m.a. of current was used. The output of the hot-wires was amplified and recorded in the same manner as for the strain-gage. Since the frequency of shedding was all that was needed, no calibration was necessary.

A cathode-ray oscilloscope was used in parallel with the recording oscillograph so that visual observation of both the oscillation of the airfoil and the shedding of vortices could be made while records were being taken. By means of the traversing mechanism and observing the output of the hot-wire on the scope, the hot-wire could be moved to the best position for any velocity and angle of attack setting for picking up the vortex frequency. This was necessary because inside the wake it was difficult to obtain any defined pattern of flow due to high turbulence. On the border of the wake the influence of the vortex formation could be felt by the hot-wire without any appreciable effect of the wake turbulence.

The accuracy of velocity measurement by means of pitot-static tube mounted in the test section ahead of the airfoil was 0.2 f.p.s.

The accuracy of setting the angle of attack with respect to the windstream direction was 1/3 degree.

The accuracy of oscillation amplitude measurement with the shunt calibrations was 0.1 degree.

At the lower angles of attack, from stall to about 15 degrees, the accuracy of vortex frequency reading was approximately 15%, while at higher angles it was approximately 3%.

V. TEST PROCEDURE

The velocity survey of the working section was accomplished by placing a pitot-static tube at 30 positions with the airfoil removed, and the results are presented in Figure 4.

The wake surveys were for angles of attack of 8°, 12° and 15°, both with the airfoil held stationary and with it oscillating. The results are presented in Figures 5 to 8.

Tuft surveys were made at angles of attack of 6°, 8°, 12°, 15° and 19°, with the airfoil stationary, and the results are presented in Figure 8a.

For the oscillation amplitude and the vortex shedding frequency measurements the following procedure was followed: The airfoil was mounted on Suspension #1, set at the desired angle of attack, and the velocity was increased slowly until the oscillation just started. The velocity was then decreased approximately 5 f.p.s. to a point where there was no longer any oscillation. With the airfoil stationary the lower hot-wire was moved into position, and by observing the pattern on the oscilloscope the best position was found for determining the vortex frequency. A record was then taken of the vortex shedding frequency. The velocity was then increased and another vortex frequency record was taken with the airfoil stationary. The airfoil was released and allowed to begin self-excited oscillation. If there was any oscillation at that particular velocity, it was allowed to reach a steady value by observing the oscilloscope. When the steady state was reached, the amplifier gain was adjusted so that the traces filled up the oscilloscope screen. The vertical gain in the oscilloscope was already adjusted so that full use of the screen corresponded to the full use of the recording tape in the oscillograph. Again the airfoil

was stopped and a calibration mark was put in the record. One of four calibration marks could be chosen, corresponding to amplitudes of approximately 1°, 3°, 7° and 10°. The airfoil was then released again and allowed to reach steady state of oscillation before a record was made of the oscillation.

The airfoil was again stopped and the velocity was increased by about 1 f.p.s., following which the procedure just described was repeated. This was done up to the point where oscillation no longer started; or, in cases where the oscillation amplitude kept increasing, the test was terminated when the amplitude was near the elastic limit of the torsion rods, which was about 15 degrees. These tests were run for angles of attack of 7°, 8°, 10°, 12°, 14°, 15°, 18°, 21°, 23°, 25°, 27° and 29°. The results of these runs are presented in Figures 9 to 20.

Similar measurements were made with Suspension #2, at angles of attack of 8°, 12°, 25°. The results are presented in Figures 26 to 28.

In order to obtain a complete set of data to show the relationship between the vortex shedding frequency of the stationary airfoil and the angle of attack, with velocity as a parameter, hot-wire frequency records were taken over a velocity range of 20 to 45 f.p.s. for angles of attack of 7°, 8°, 10°, 12°, 14°, 15°, 18°, 21°, 23°, 25°, 27° and 29°. Results of these runs are presented in Figures 29 to 35.

By manipulating the hot-wire mounted from the top of the test section, the point of flow separation on the upper surface was found for angles of attack of 9°, 12°, 15°, 18° and 21°. A scale was mounted over the top of the airfoil, with zero at the leading edge, so that point of separation could be measured with respect to the leading edge. Results are presented in Figure 36.

Finally, to study the shedding phenomenon while the airfoil was oscillating, and to examine the phase relation of the shedding with the oscillation, simultaneous records of the strain-gage and of the hot-wires mounted on the airfoil were taken for angles of attack of 8°, 10° and 18°. For each angle of attack and velocity setting a record was first taken with the oscillation traces and the shedding traces from the leading edge put on the same tape, so that the phase relations could be examined. For the same configuration another record was made with the oscillation traces and the shedding traces taken behind the trailing edge. Results of these tests are presented in Figure 37.

VI. EXPERIMENTAL RESULTS

The results of the velocity survey, shown in Figure 4, indicates that the maximum velocity variation was about 1.6% in the test section.

The wake surveys are presented in Figures 5 to 8. Figures 5 and 6 show that the oscillating airfoil produced a wake of nearly the same width as the stationary one. A comparison of Figure 7 with Figure 8 indicates that the wake for 12 degrees of angle of attack was wider than that for 15 degrees.

The tuft surveys, as presented in Figure 8a, show that the flow was not strictly two-dimensional.

Figures 9 to 20 give the results of the oscillation amplitude and the shedding frequency as a function of velocity for angles of attack of 7°, 8°, 10°, 12°, 14°, 15°, 18°, 21°, 23°, 25°, 27° and 29°, using Suspension #1, which had a frequency of approximately 12 c.p.s. These show that for angles of attack below 14° there was apparently no upper limit of velocity at which self-excited oscillations occurred. For angles of attack higher than 14° there were upper limits, and the range of velocity in which oscillations started became less as the angle of attack was increased. It may also be seen that for the higher angles of attack the vortex shedding frequency within the oscillation range was near the natural frequency of the oscillating system.

The plots of velocity range in which self-excited oscillation occurred as a function of angle of attack are given in Figure 21. The plots of vortex frequency range in which oscillation occurred as a function of angle of attack are given in Figures 22 and 23.

The maximum amplitude of oscillation and the corresponding velocity and vortex frequency for the stationary airfoil as a function of angle of attack are given in Figure 24. Oscillation amplitudes as a function of angle of attack with the velocity as a parameter are plotted in Figure 25.

Due to lack of time a thorough study of the oscillation phenomena using Suspension #2 could not be made, although limited results were obtained and are presented in Figures 26 to 28. Also, the limited velocity range of the windtunnel restricted the scope of investigation using the stiffer suspension.

Figures 29 to 33 give vortex frequency of the stationary airfoil as a function of velocity for angles of attack of 7°, 8°, 23°, 27° and 29°. These show that the frequencies are quite irregular just above stall, but are regular for the higher angles.

Figures 34 and 35 show vortex shedding frequency as a function of $\sin\alpha$ at different velocities. It is seen that, instead of following a linear relation as indicated by Tyler's formula given in Reference 3, $\frac{nb \sin\alpha}{V} = K$, the shedding frequency decreases at lower angles of attack. At the higher angles the value of K ranges between 0.112 and 0.178, which is in fair agreement with the values given in Reference 3. Tyler gives an average value for K of 0.15 for airfoils, while Blenk, Fuchs and Liebers give an average value of 0.21.

Results of the measurement of point of separation are given in Figure 36, which shows that the separation point on the upper surface is fixed for the range of angles of attack from stall to 14°, and shifts

to a new fixed position from 15° on.

The results with the hot-wires attached to the oscillating airfoil and measuring shedding and oscillation simultaneously are given in Figure 37. These are discussed in detail in the next section.

VII. DISCUSSION

The factors affecting the oscillation of a system like the airfoil used in this experiment are the following: the moment of inertia of the entire system, the torsional rigidity of the suspension system, the aerodynamic damping moment, and the torsional moment caused by the vortex shedding. The moment of inertia of the system is constant if the system is at rest, but is increased by an "additional apparent moment of inertia" when it is in motion in a fluid.. Assuming the airfoil itself to be very rigid compared to the torsion rods, which is true in this case, the torsional rigidity of the system depends on the rigidity of the torsion rods, and is therefore constant. The aerodynamic damping on an oscillating airfoil depends on the angle of attack, the frequency and amplitude of oscillation and the velocity of the airstream. Glauert shows in Reference 4 that for an oscillating lifting wing this damping moment is positive except for suspension point further forward than the 25% chord point.

If the airfoil is initially at rest, energy must be put into the system to set it into oscillation. The mechanism which puts energy into the system is the periodic shedding of vortices. Experimental results show that no oscillation occurred for angles of attack less than 6 degrees. Investigation with the hot-wire also showed that there was no shedding of vortices for angles of attack less than 6 degrees. The lift curve for the NACA 0006 airfoil in Figure 3 shows that the curve begins to deviate from a straight line after 6 degrees. The amount of energy put in must balance the

dissipation due to damping in order to maintain the oscillation. It may be expected that the energy input due to the shedding of vortices would be a maximum when the shedding frequency is equal to the oscillation frequency. At this point, if the dissipation due to damping is less than the energy input, oscillation would occur and maintain itself. However, it is conceivable that at a particular angle of attack of the airfoil and a particular velocity when the shedding frequency equals the natural frequency of the system the energy input is not sufficient, due to the low velocity, to start any oscillation. It may be seen from Figure 34 that for an angle of attack of 8^{o} the velocity at which the shedding frequency equals 12 is very low, and Figure 10 shows that there was no oscillation at this point. At higher angles of attack, a shedding frequency of 12 requires a higher velocity, which may be sufficient to start an oscillation. Results at the higher angles of attack, as presented in Figures 13 to 20, show that oscillations start when the ratio of shedding frequency to natural frequency is near 1. If the velocity is increased it may be expected that the shedding frequency increases and becomes out of phase with the natural frequency, while the damping moment, at the same time, is increased due to the increase in velocity, so that oscillation will no longer start. Results given in Figures 13 to 20 show this to be the case.

The results at the lower angles of attack, as given in Figures 9 to 12, show that there was no upper limit to the range of velocity in which self-excited oscillation occurred, even when the shedding frequency with the stationary airfoil was as high as 4 times the

natural frequency. And once the oscillation began it rapidly built up to very high amplitudes. This leads one to the conjecture that at these lower angles of attack the shedding frequency, once the oscillation is started, is controlled by the oscillation frequency itself, and no longer by the velocity and the stationary angle of attack. Furthermore, it is obvious that at the lower angles of attack the airfoil must go into the unstalled state during part of the cycle of oscillation. If an airfoil is stalled and unstalled periodically, the change in the circulation and, consequently, the shedding of vortices must also be periodic and have the same frequency as the oscillation. To show that this was the case at the lower angles of attack, hot-wires were mounted on the oscillating airfoil to study the flow condition over the airfoil during the oscillation. Figure 37 shows the results of this study.

Figure 37a shows two traces, the sinusoidal one being the oscillation of the airfoil and the other one the flow condition over the airfoil just behind the leading edge. The amplitude of oscillation in this case was 6.5°, so that at the upper end of the travel the airfoil was at an angle of attack of 14.5° and at the lower end of the travel it was at 1.5°. In the trace of the hot-wire response it is seen that from point 1 to point 2 it is straight and level. Point 1 corresponds to an angular position of 1.5° and point 2 corresponds to 13.5°. Thus, the record indicates that between 1.5° and 13.5° the flow over the airfoil was smooth. But at point 2 the smooth flow broke down sharply, indicating the shedding of a vortex. This vortex formation began just before the airfoil started on its downward swing. Figure 37b, which

gives the traces of the oscillation and the flow condition behind the trailing edge, indicates that at point 1 the flow at the trailing edge took a sudden increase in speed due to the shedding of the vortex. Thus it is seen that one vortex each was shed from the leading and trailing edges during each cycle of oscillation. Therefore, in the case of lower angle of attack, when during part of the cycle the airfoil was in the unstalled state, the oscillation frequency controlled the shedding frequency. The shedding of the vortices in turn maintained the oscillation, since the moment produced by the shedding was in phase with the oscillation. These results substantiate the statement made in Reference 1, p. 25, that the oscillating airfoil must control the vortex frequency over a very large range of velocities.

At the higher angles of attack the airfoil was apparently stalled throughout the cycle of oscillation, as indicated results given in Figure 37d, which shows the oscillation and flow condition over the airfoil at an angle of attack of 18° and oscillation amplitude of 7.0°. Figure 37c shows an intermediary case, in which the unstalled region was less extended than in the case represented by Figure 37a.

VIII. CONCLUSION

At the higher angles of attack the oscillation was controlled by the shedding of vortices, and resonance between vortex shedding and oscillation was apparent. The oscillation phenomena at the lower angles of attack need be further investigated. The exciting moments and the damping moments should be examined quantitatively in order to arrive at a more definite correlation of vortex shedding to torsional oscillation.

IX. REFERENCES

1. Dunn and Finston, "Self-excited Oscillations of Airfoils"
Report in Final Fulfillment of Contract NAW 2329, April, 1945
California Institute of Technology. Confidential

2. Levy, "Self-excited Torsional Oscillations of An Airfoil"
Thesis, California Institute of Technology, June, 1945. Confidential

3. Goldstein, "Modern Developments in Fluid Dynamics"
Oxford, 1938. Vol. II, Chapt. XIII

4. Glauert, "The Force and Moment on an Oscillating Airfoil"
Aeronautical Research Committee, Reports and Memoranda
No. 1242, 1930

X. FIGURES AND GRAPHS

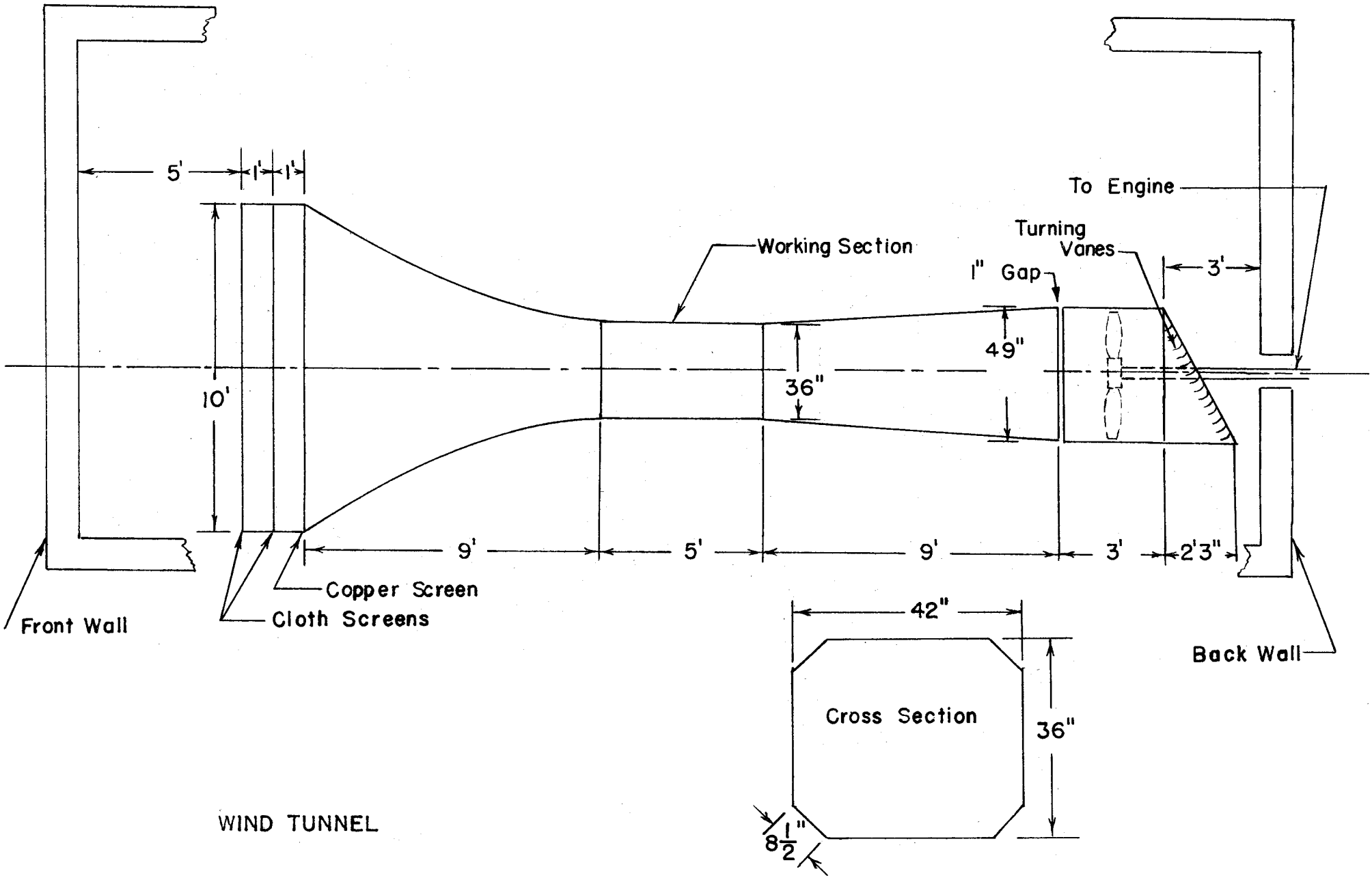

WIND TUNNEL

FIG. 1

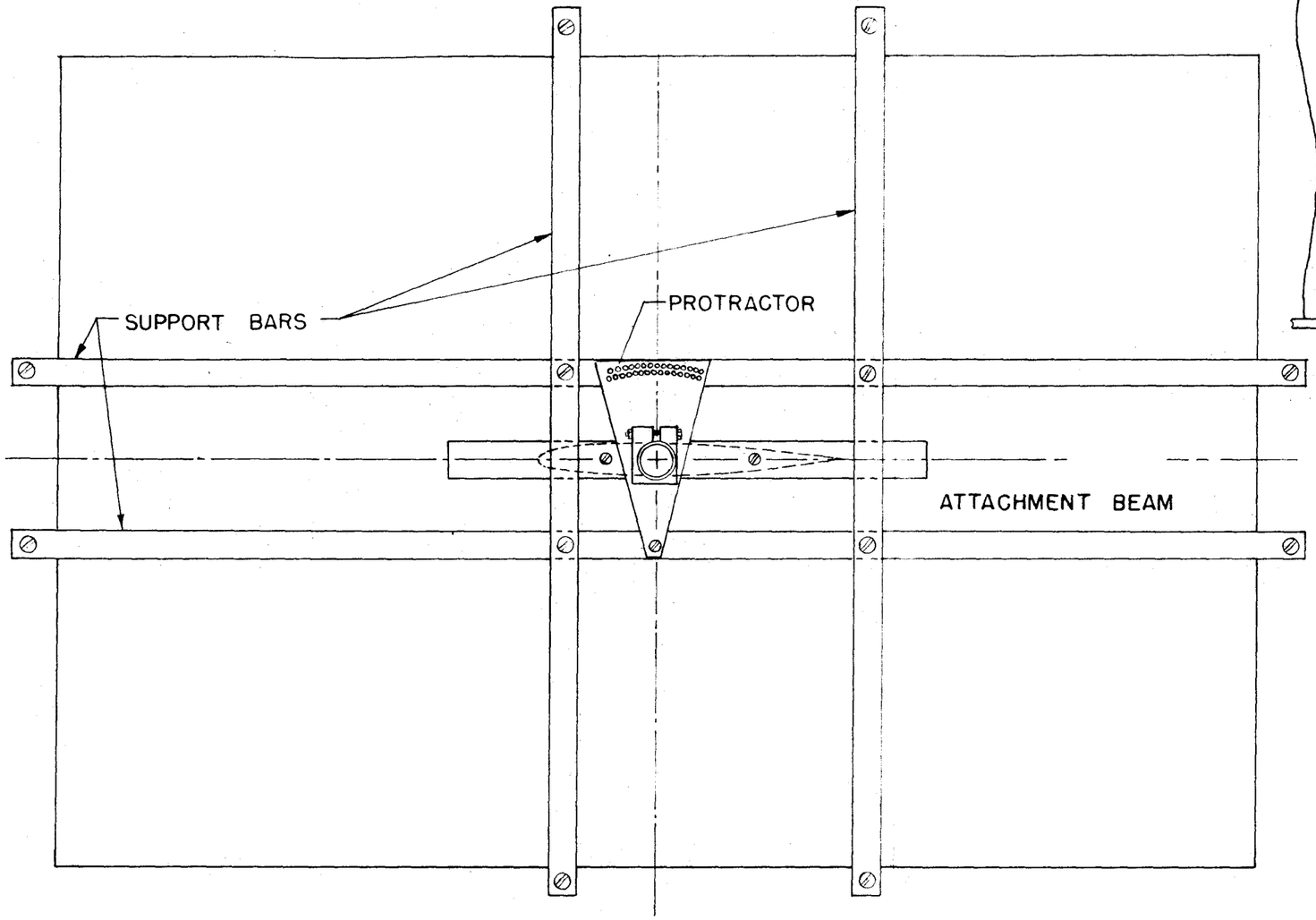

SIDE VIEW OF SUPPORT SYSTEM

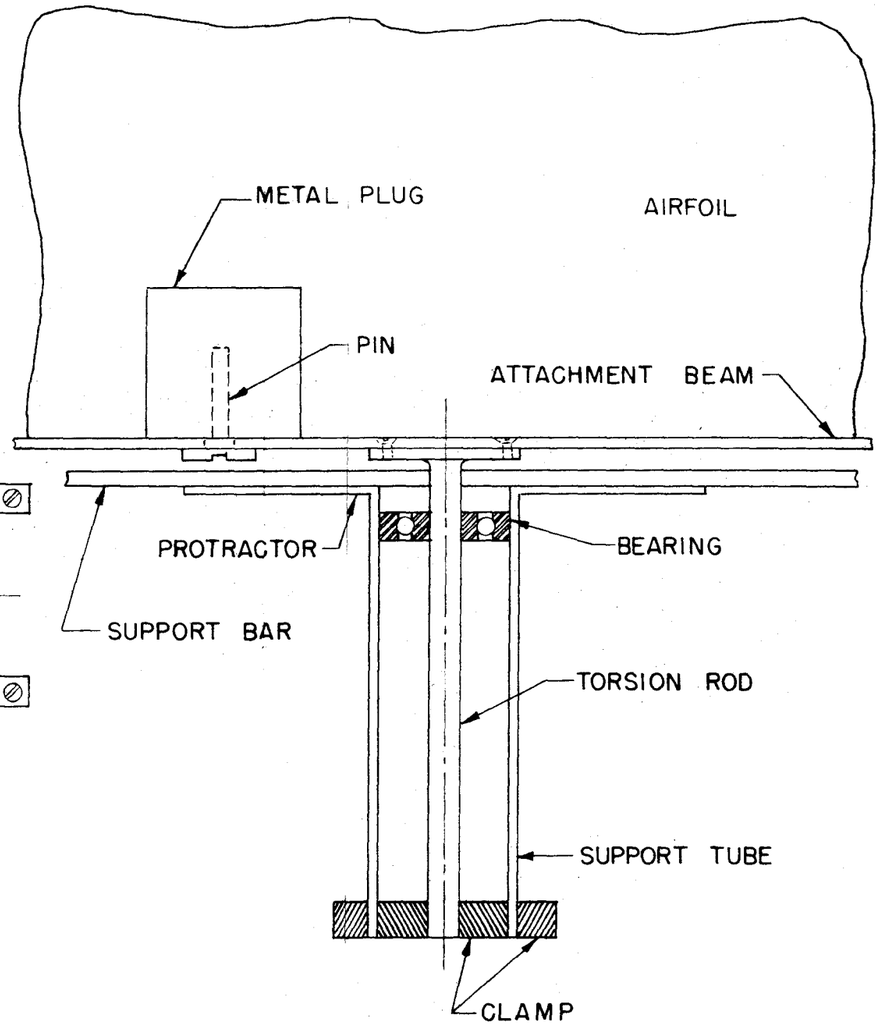

TOP VIEW OF TORSION ROD SUPPORT SYSTEM

TORSIONAL OSCILLATION SUSPENSION

FIG. 2

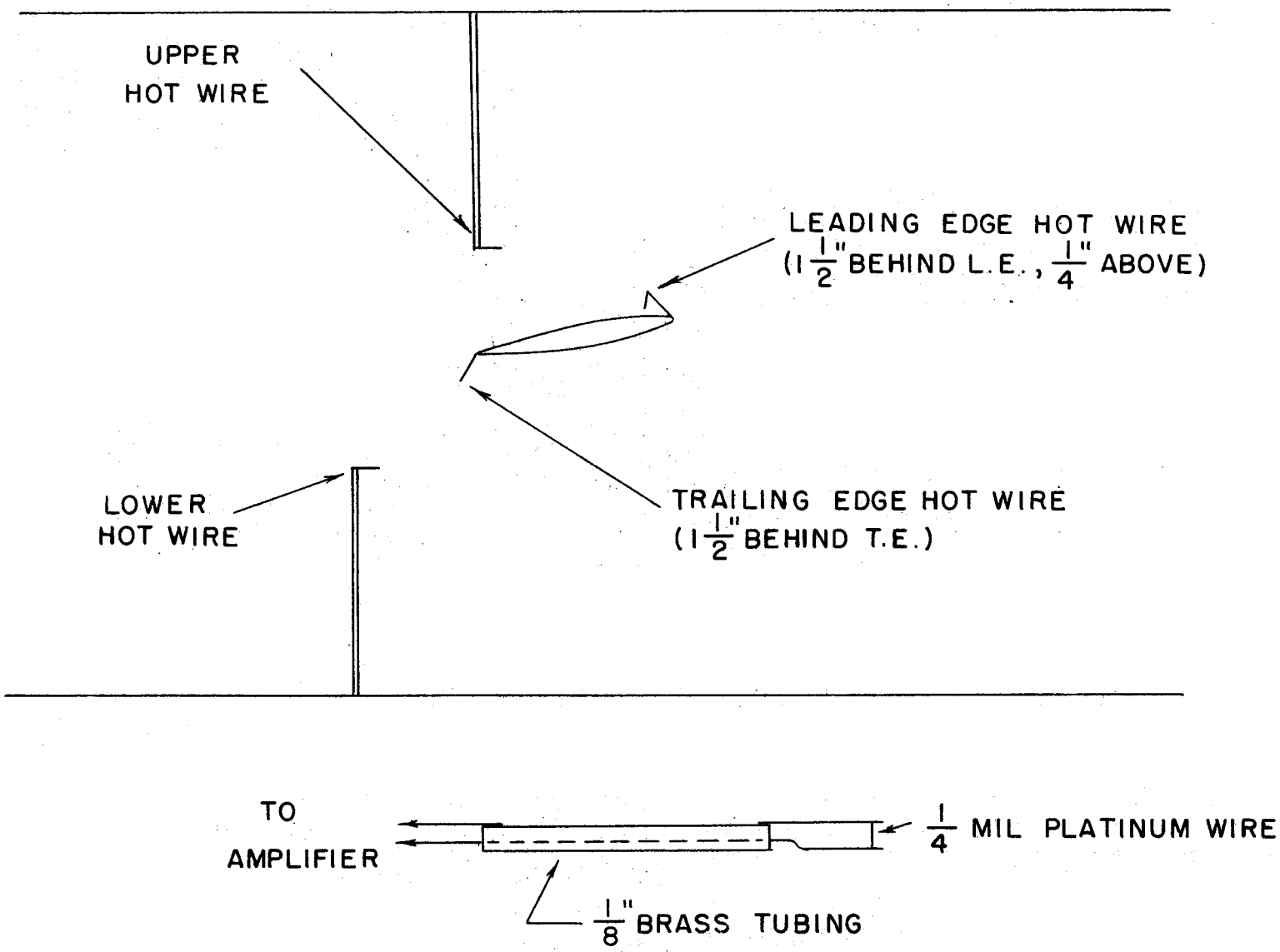
UPPER
HOT WIRE
LEADING EDGE HOT WIRE
(1 1/2" BEHIND L.E., 1/4" ABOVE)
LOWER
HOT WIRE
TRAILING EDGE HOT WIRE
(1 1/2" BEHIND T.E.)
TO
AMPLIFIER
1/4 MIL PLATINUM WIRE
1/8" BRASS TUBING

FIG. 2a

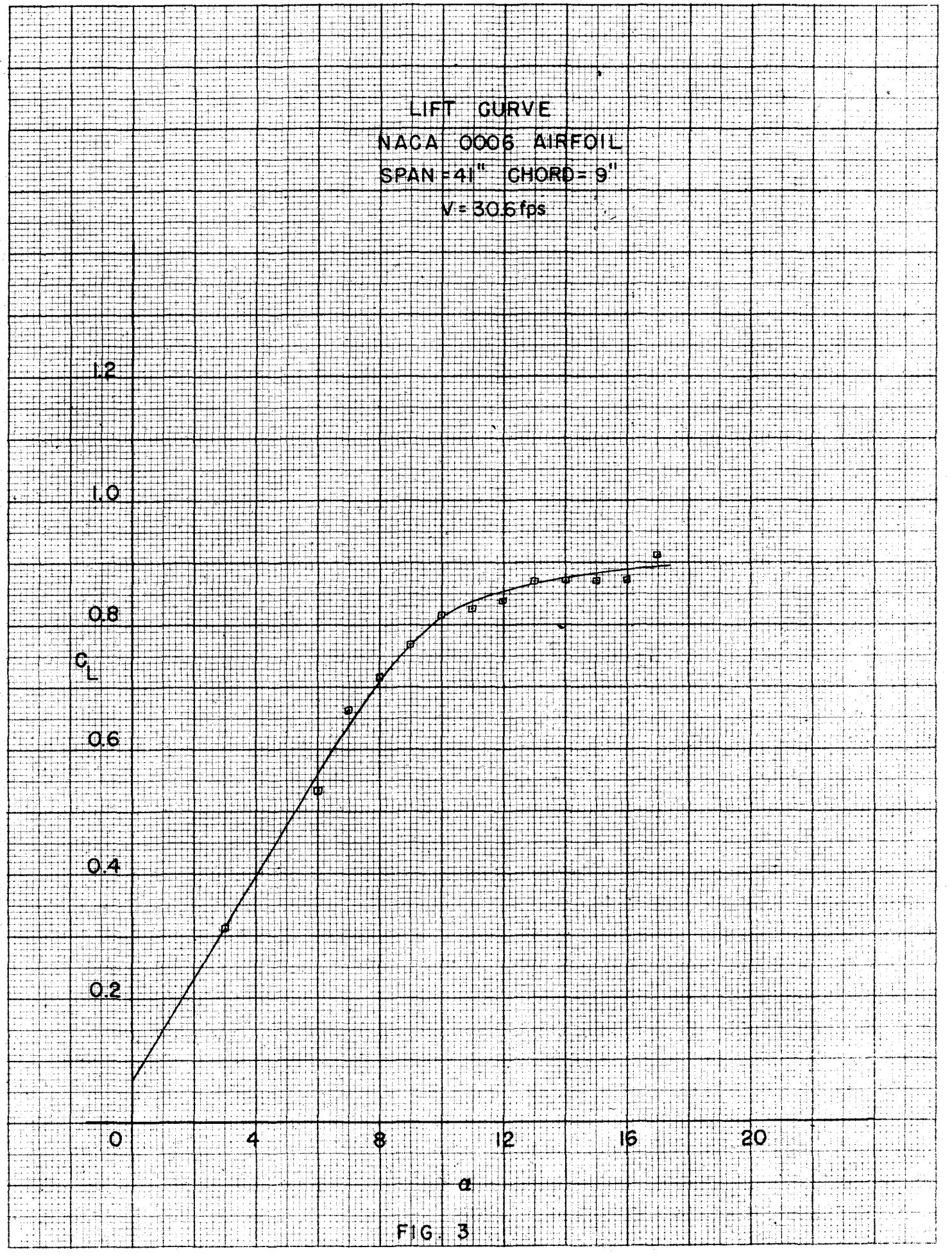
LIFT CURVE
NACA 0006 AIRFOIL
SPAN = 41" CHORD = 9"
V = 30.6 fps
1.2
1.0
0.8
C_L
0.6
0.4
0.2
0
4
8
12
16
20
α

FIG. 3

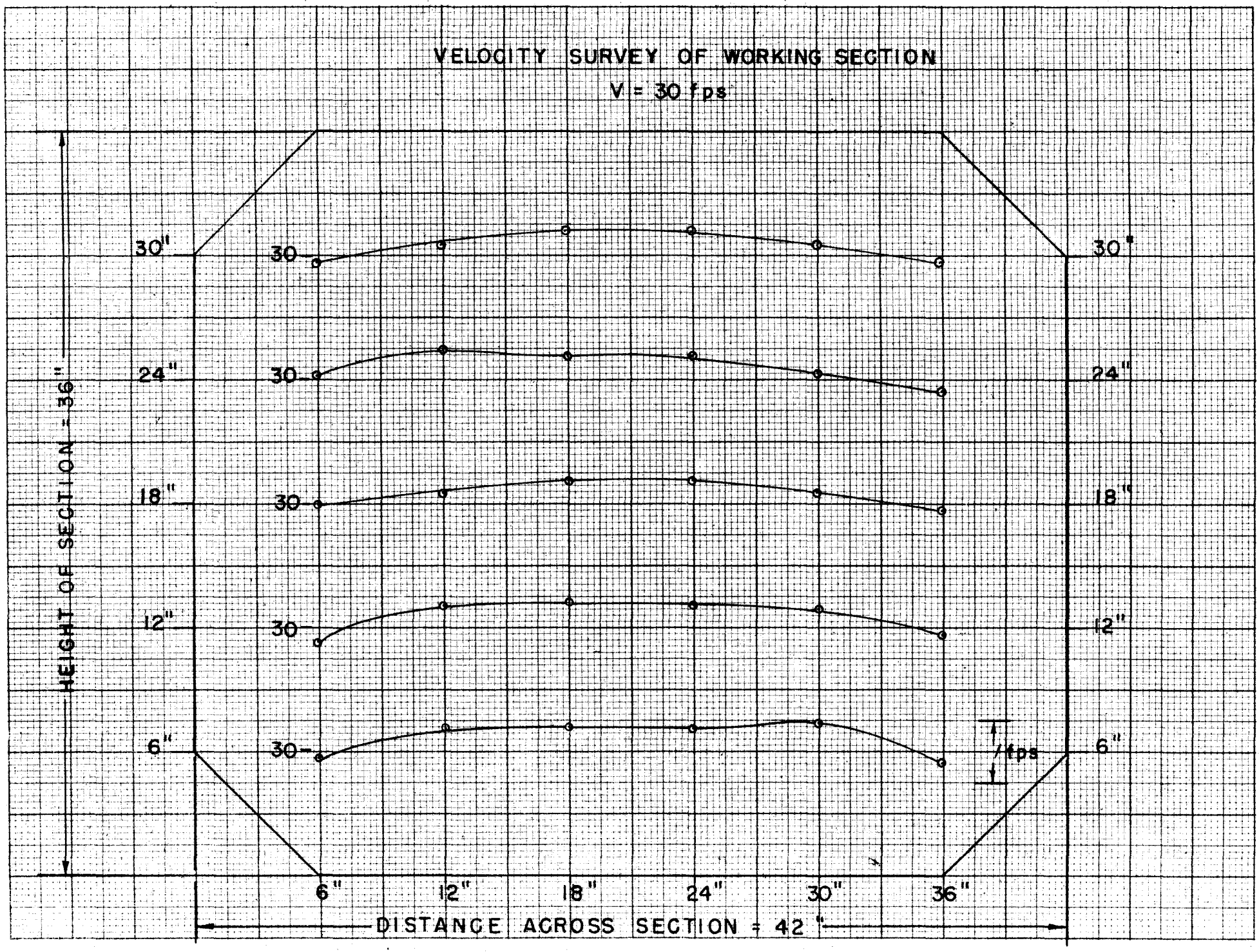
VELOCITY SURVEY OF WORKING SECTION
V = 30 fps
HEIGHT OF SECTION = 36"
DISTANCE ACROSS SECTION = 42"
30"
24"
18"
12"
6"
30
1 fps
6"
12"
18"
24"
30"
36"

FIG. 4

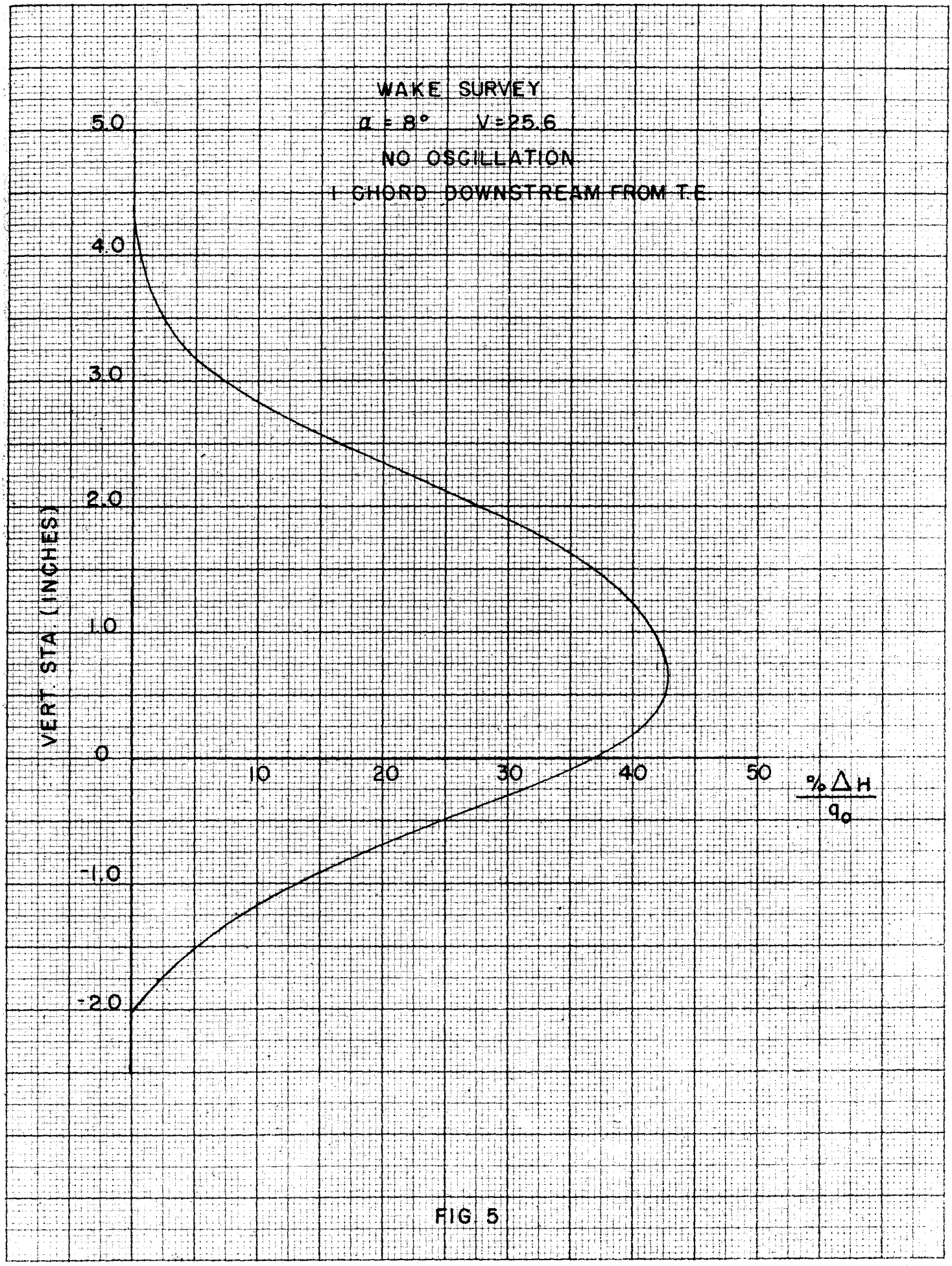
WAKE SURVEY
α = 8° V = 25.6
NO OSCILLATION
1 CHORD DOWNSTREAM FROM T.E.
5.0
4.0
3.0
2.0
1.0
0
-1.0
-2.0
VERT. STA. (INCHES)
10
20
30
40
50
% ΔH / q0

FIG. 5

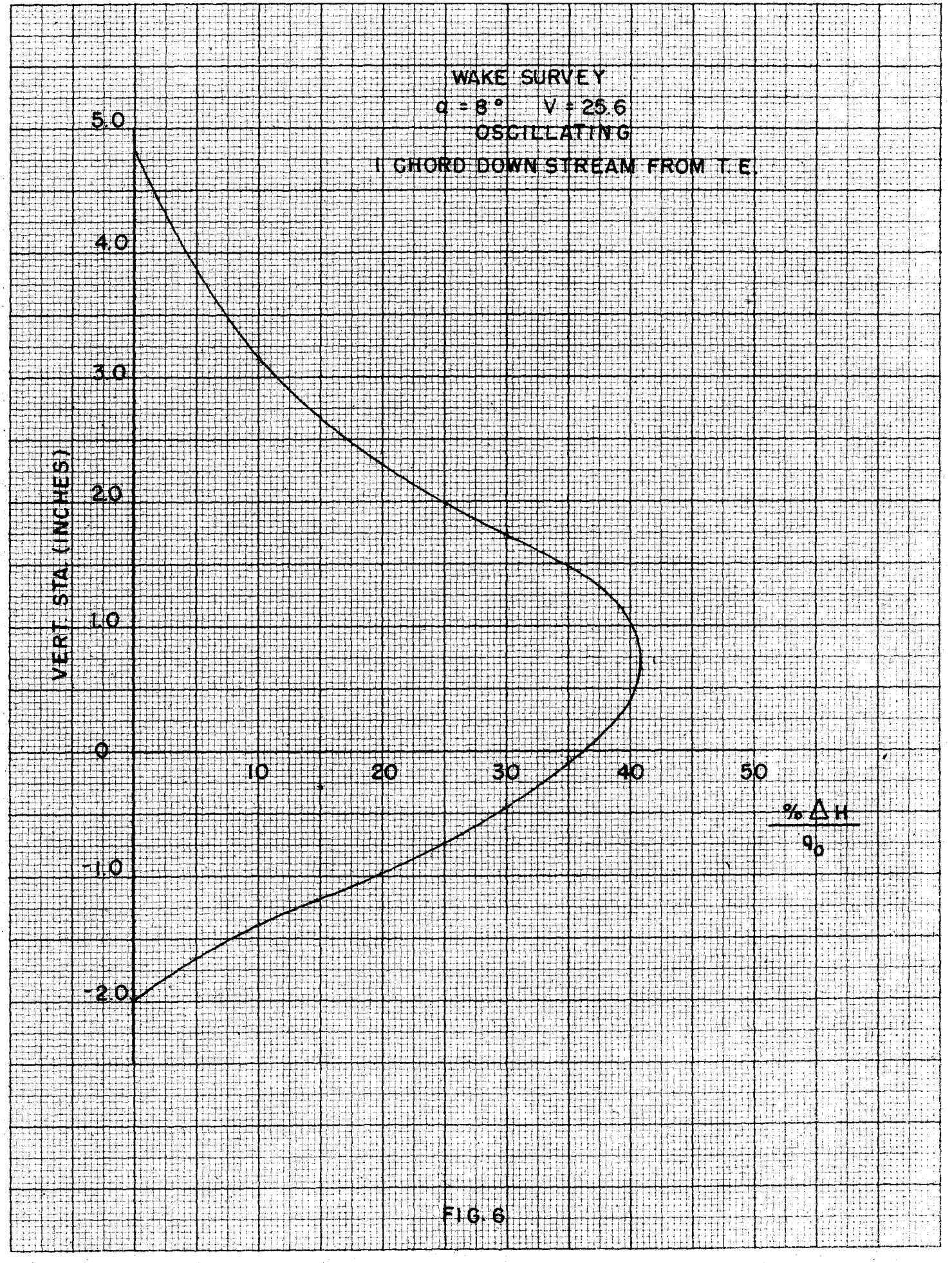
WAKE SURVEY
α = 8° V = 25.6
OSCILLATING
1 CHORD DOWN STREAM FROM T.E.
VERT. STA. (INCHES)
5.0
4.0
3.0
2.0
1.0
0
-1.0
-2.0
10
20
30
40
50
% Δ H / q0

FIG. 6

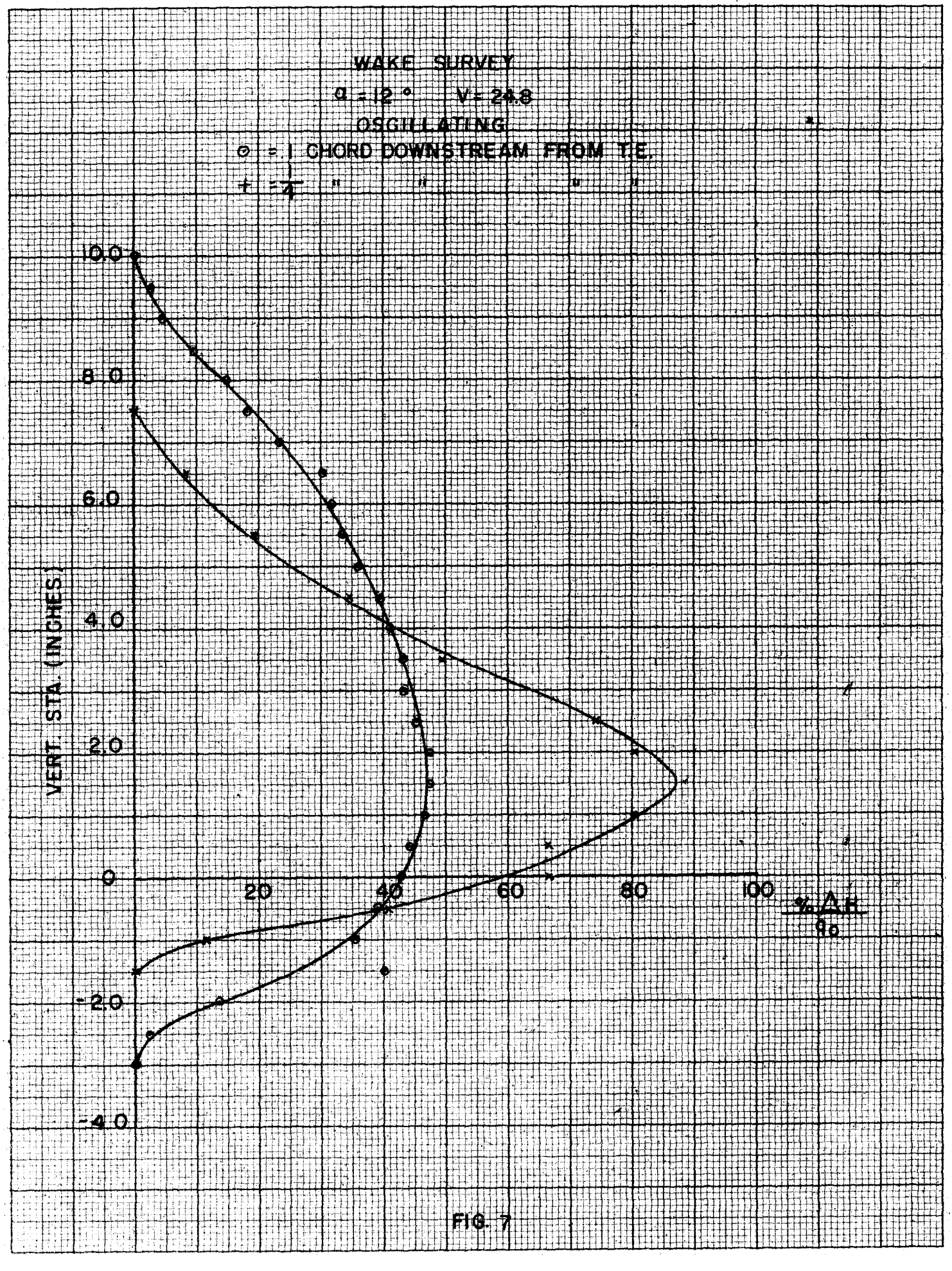
WAKE SURVEY
α = 12° V = 24.8
OSCILLATING
⊙ = 1 CHORD DOWNSTREAM FROM T.E.
+ = 1/4 " " " " "
10.0
8.0
6.0
4.0
2.0
0
-2.0
-4.0
VERT. STA. (INCHES)
20
40
60
80
100
% ΔP/q

FIG. 7

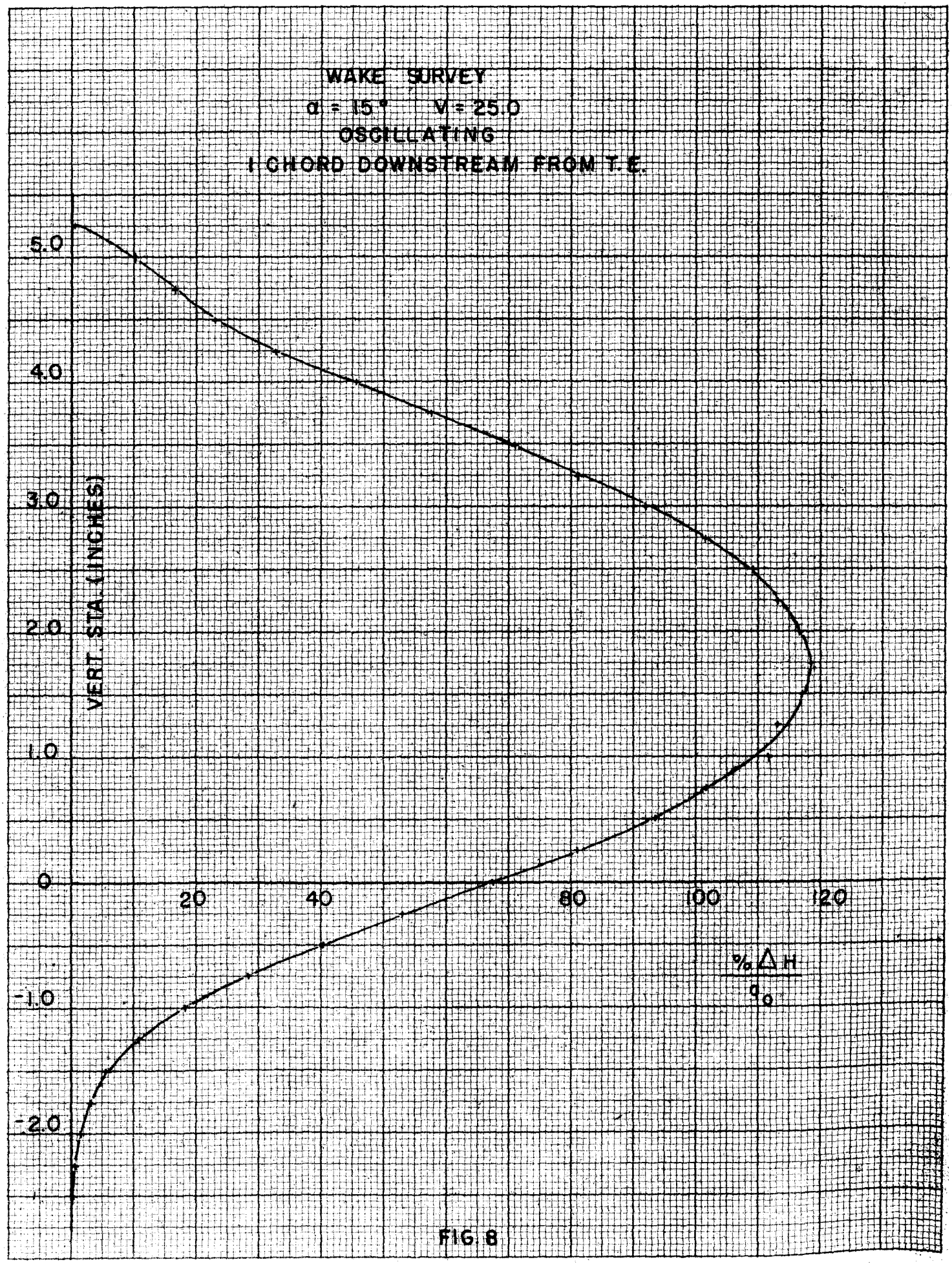
WAKE SURVEY
α = 15° V = 25.0
OSCILLATING
1 CHORD DOWNSTREAM FROM T.E.
5.0
4.0
3.0
2.0
1.0
0
-1.0
-2.0
VERT. STA. (INCHES)
20
40
80
100
120
% Δ H / q0

FIG. 8

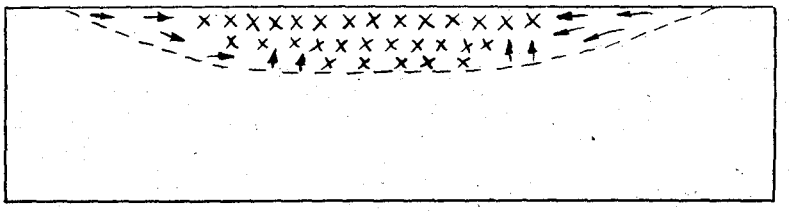

$\alpha = 6°$

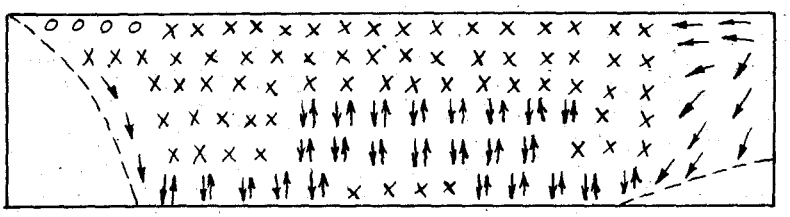

$\alpha = 8°$

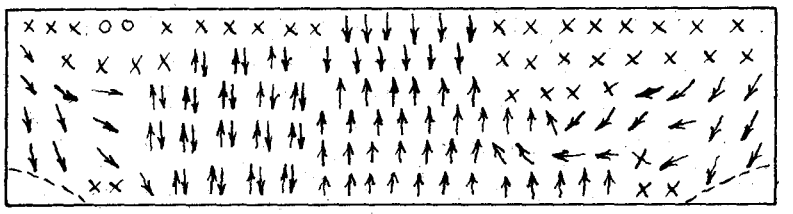

$\alpha = 12°$

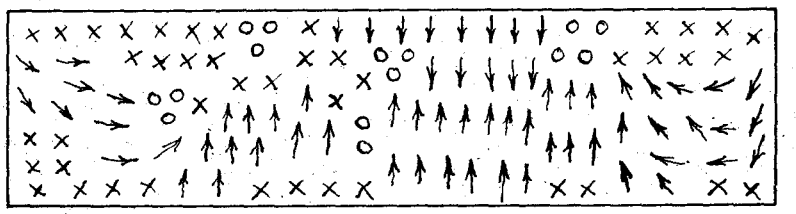

$\alpha = 15°$

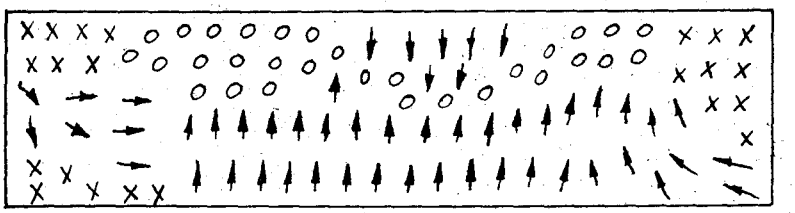

$\alpha = 19°$

LEGEND

→ STEADY FLOW

⇄ OSCILLATING FLOW

X TURBULENT FLOW

O STAGNANT

FIG. 8a

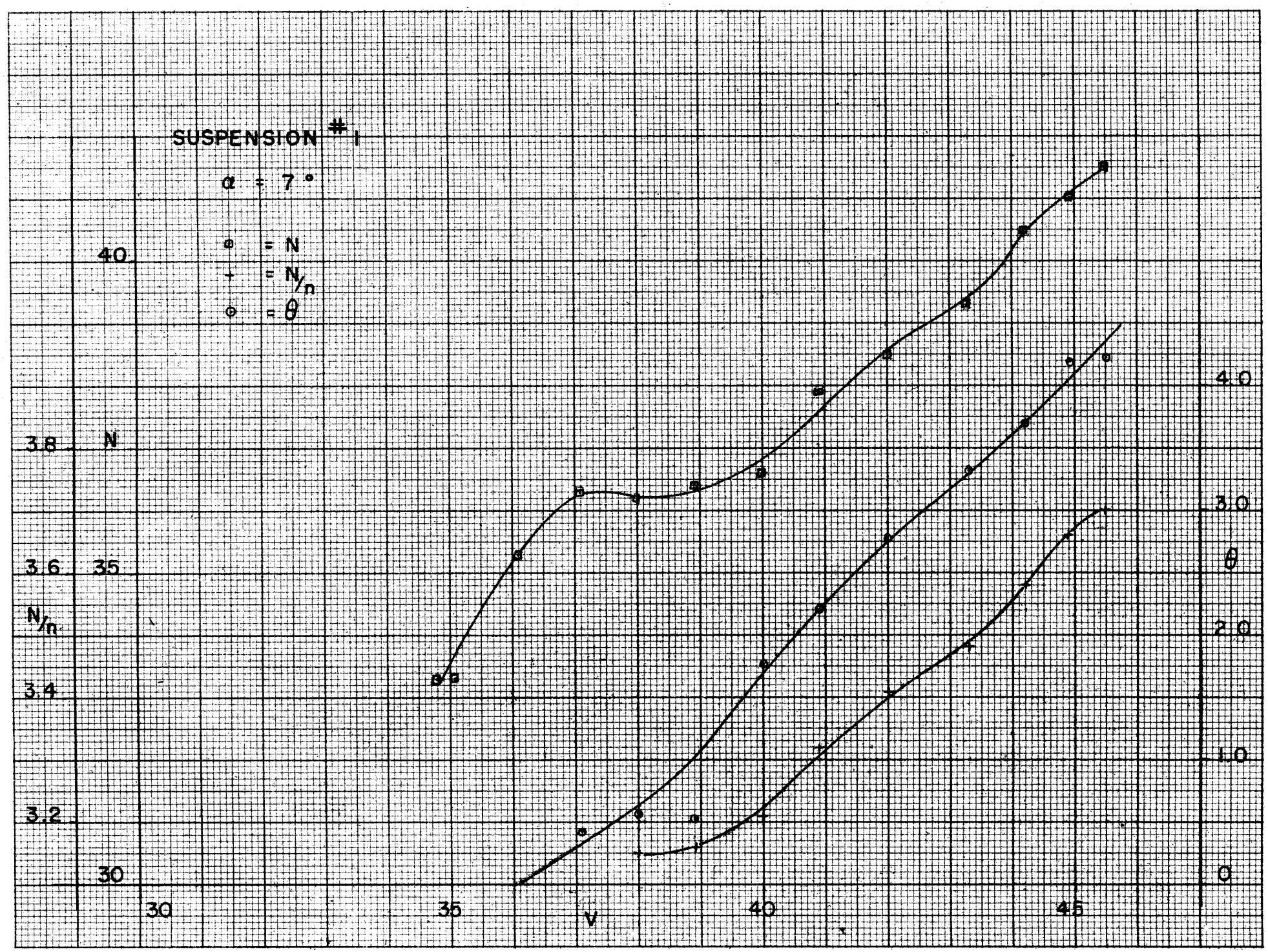
SUSPENSION # 1
α = 7°
⊗ = N
+ = N/n
⊙ = θ
40
N
3.8
35
3.6
N/n
3.4
3.2
30
30
35
V
40
45
4.0
3.0
θ
2.0
1.0
0

FIG. 9

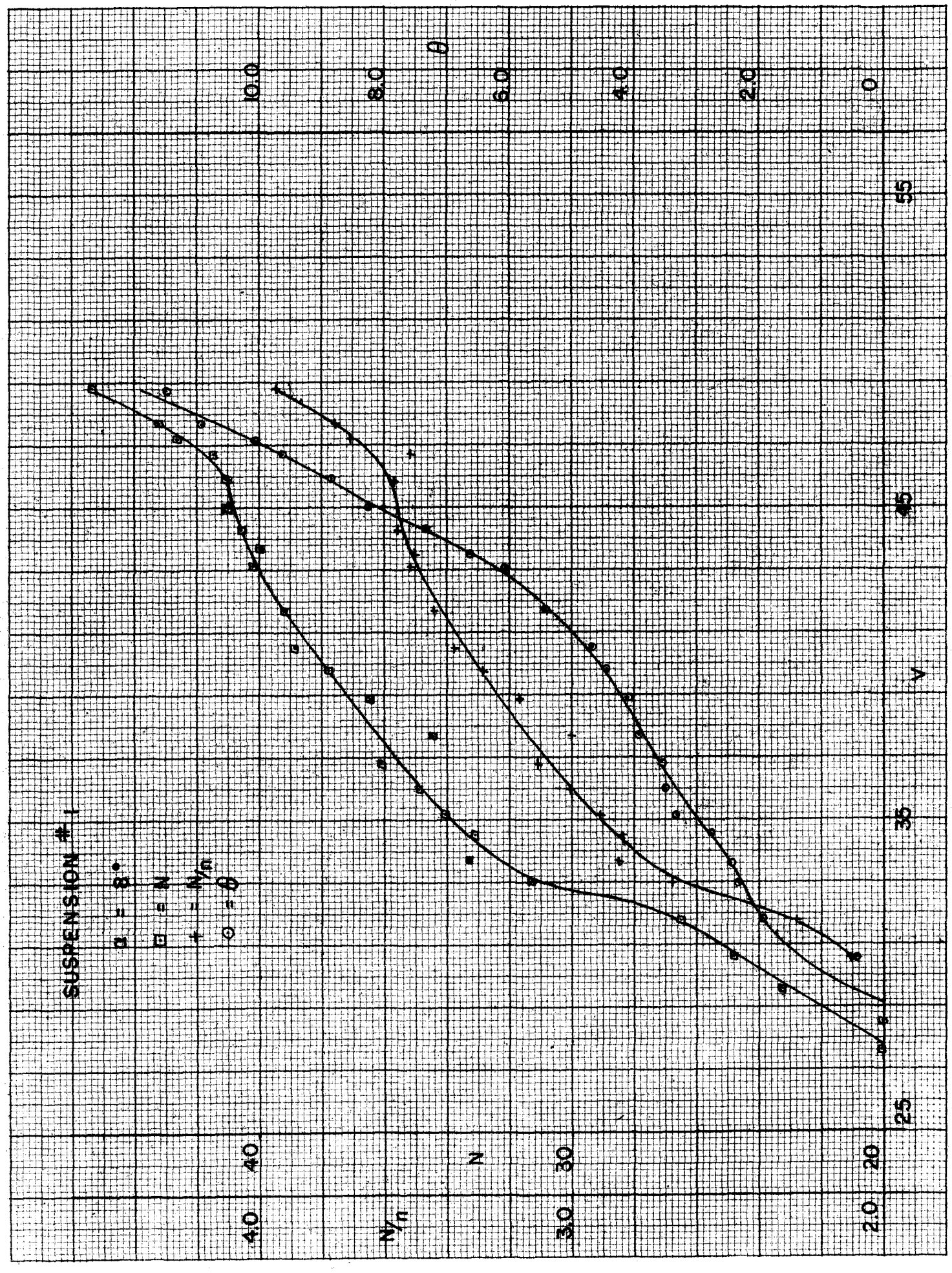

FIG. 10

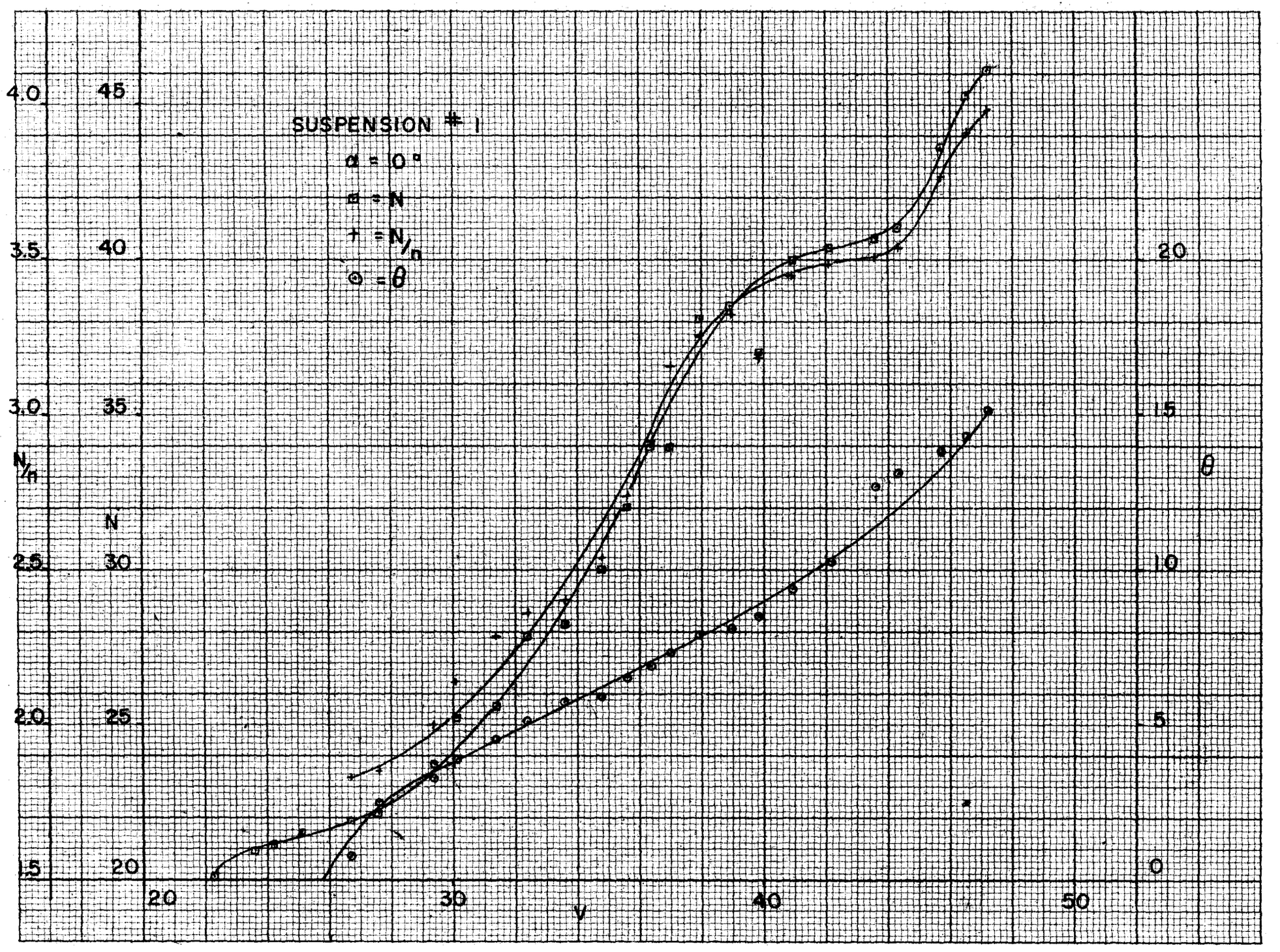
SUSPENSION # 1
α = 10°
□ = N
+ = N/n
⊙ = θ
4.0
3.5
3.0
2.5
2.0
1.5
N/n
45
40
35
30
25
20
N
20
30
40
50
V
20
15
10
5
0
θ

FIG. 11

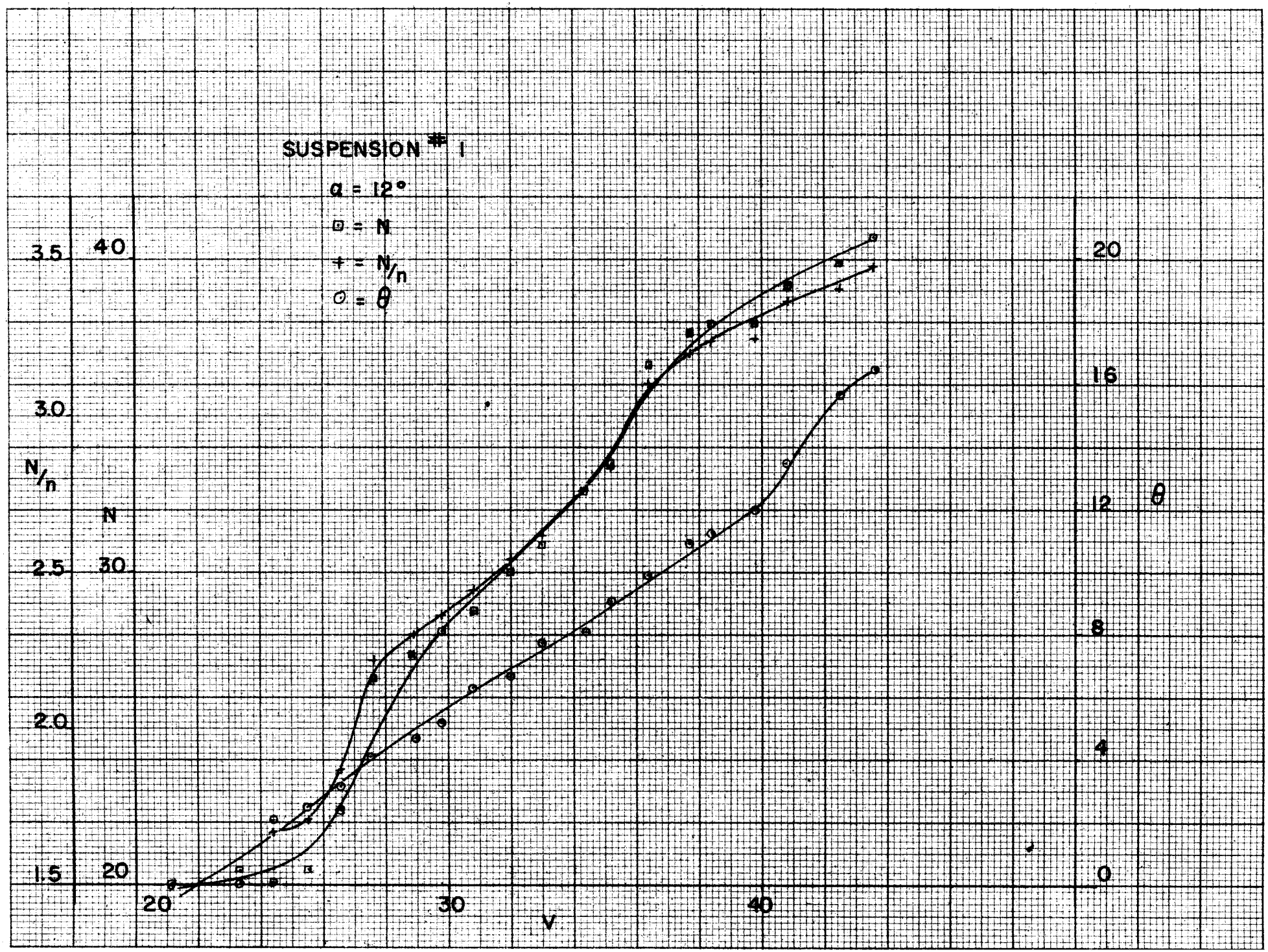
SUSPENSION # 1
α = 12°
⊡ = N
+ = N/n
⊙ = θ
3.5
40
3.0
N/n
N
2.5
30
2.0
1.5
20
20
30
40
V
20
16
12
θ
8
4
0

FIG. 12

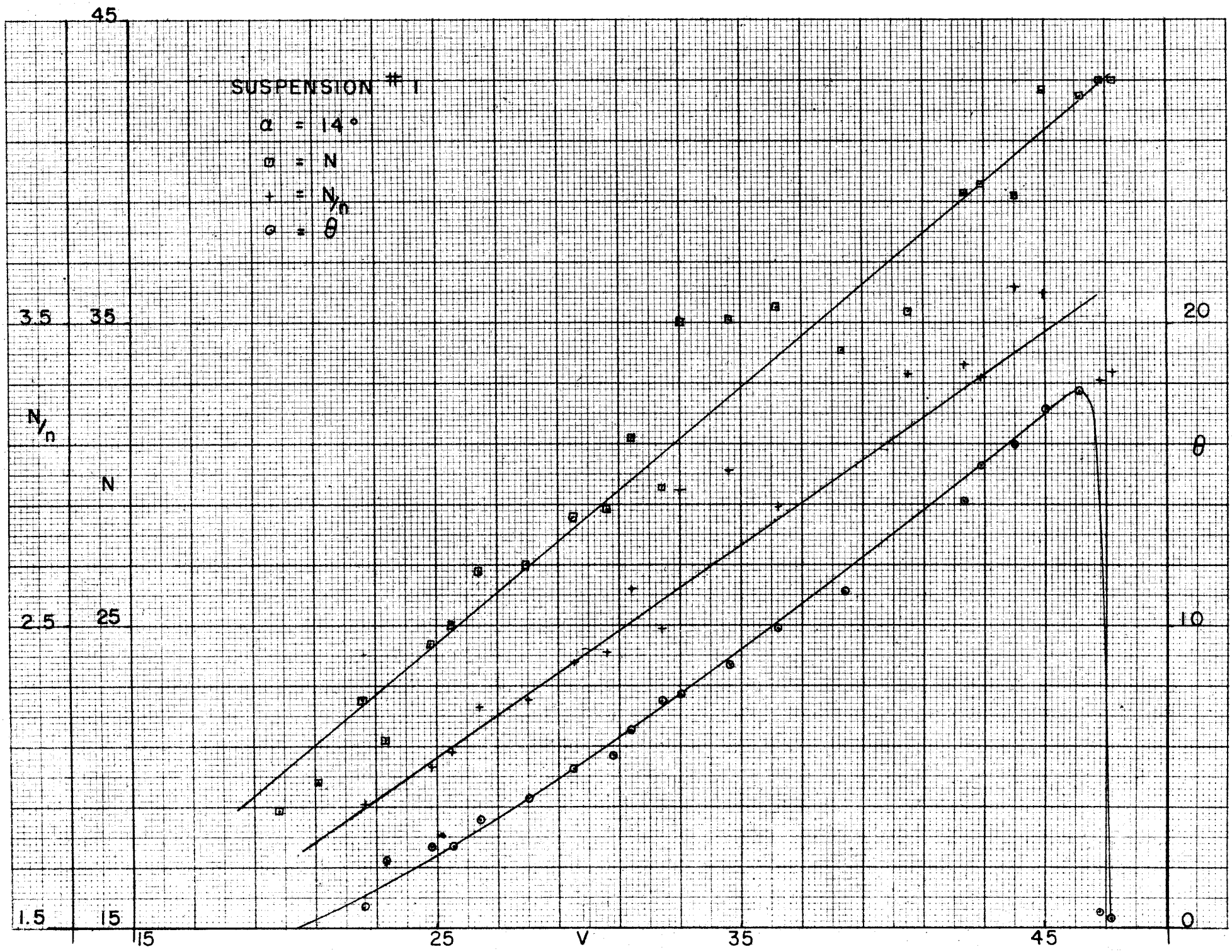
SUSPENSION # 1
α = 14°
□ = N
+ = N/n
○ = θ
45
35
25
15
3.5
2.5
1.5
N/n
N
20
10
0
θ
15
25
V
35
45

FIG. 13

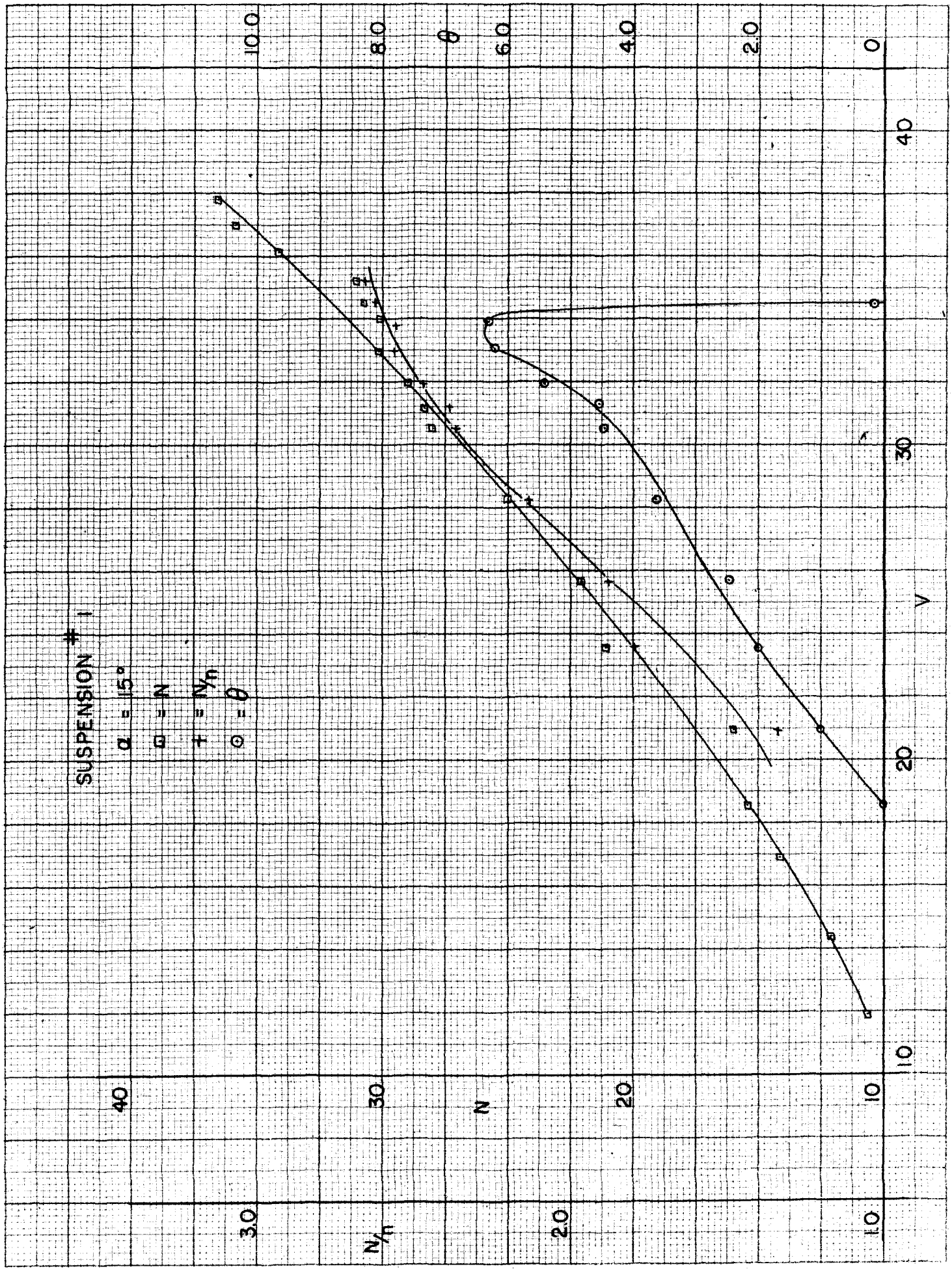

FIG. 14

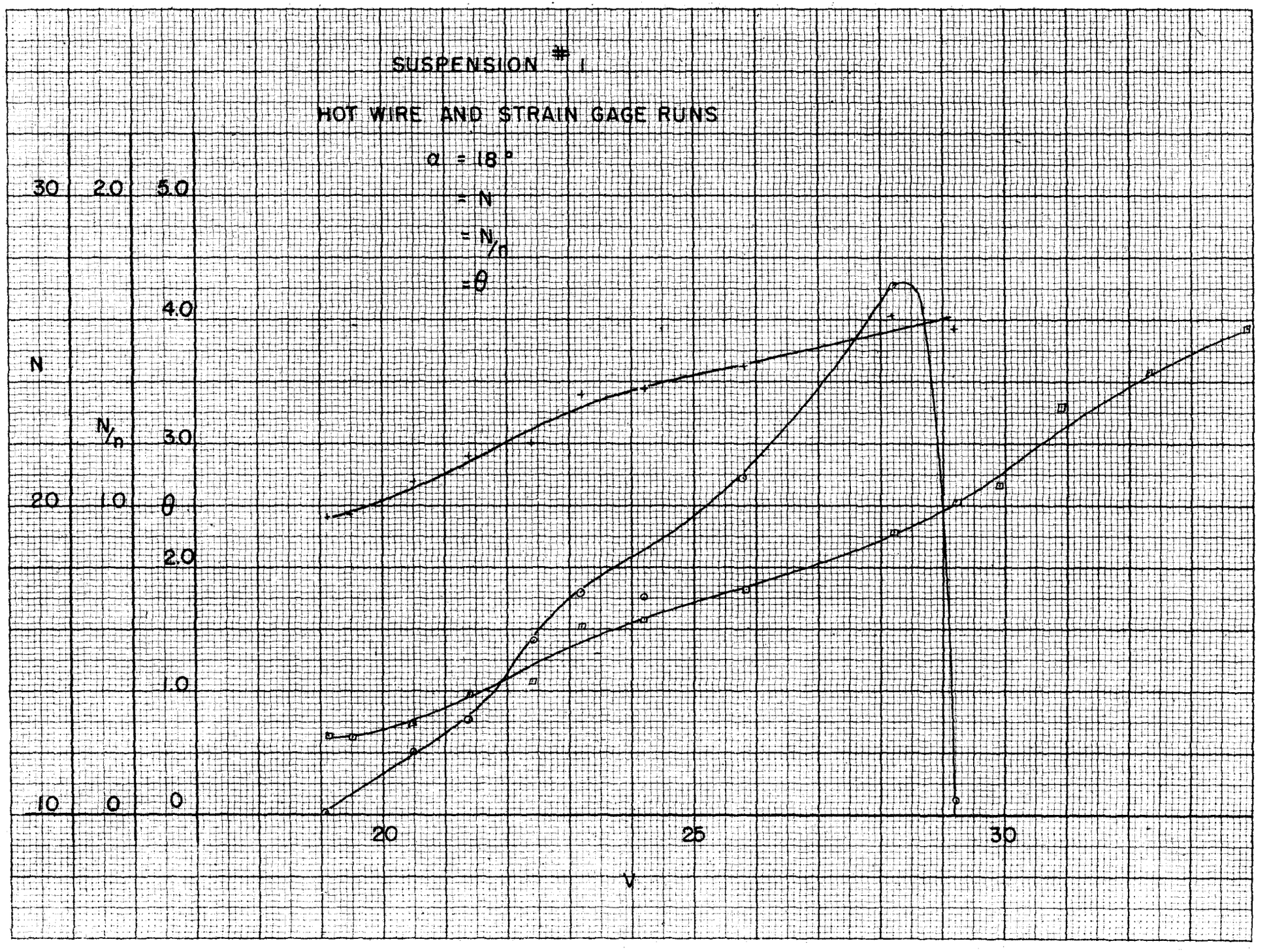
SUSPENSION # 1
HOT WIRE AND STRAIN GAGE RUNS
α = 18°
= N
= N/n
= θ
30
2.0
5.0
4.0
N
N/n
3.0
20
1.0
θ
2.0
1.0
10
0
0
20
25
30
V

FIG. 15

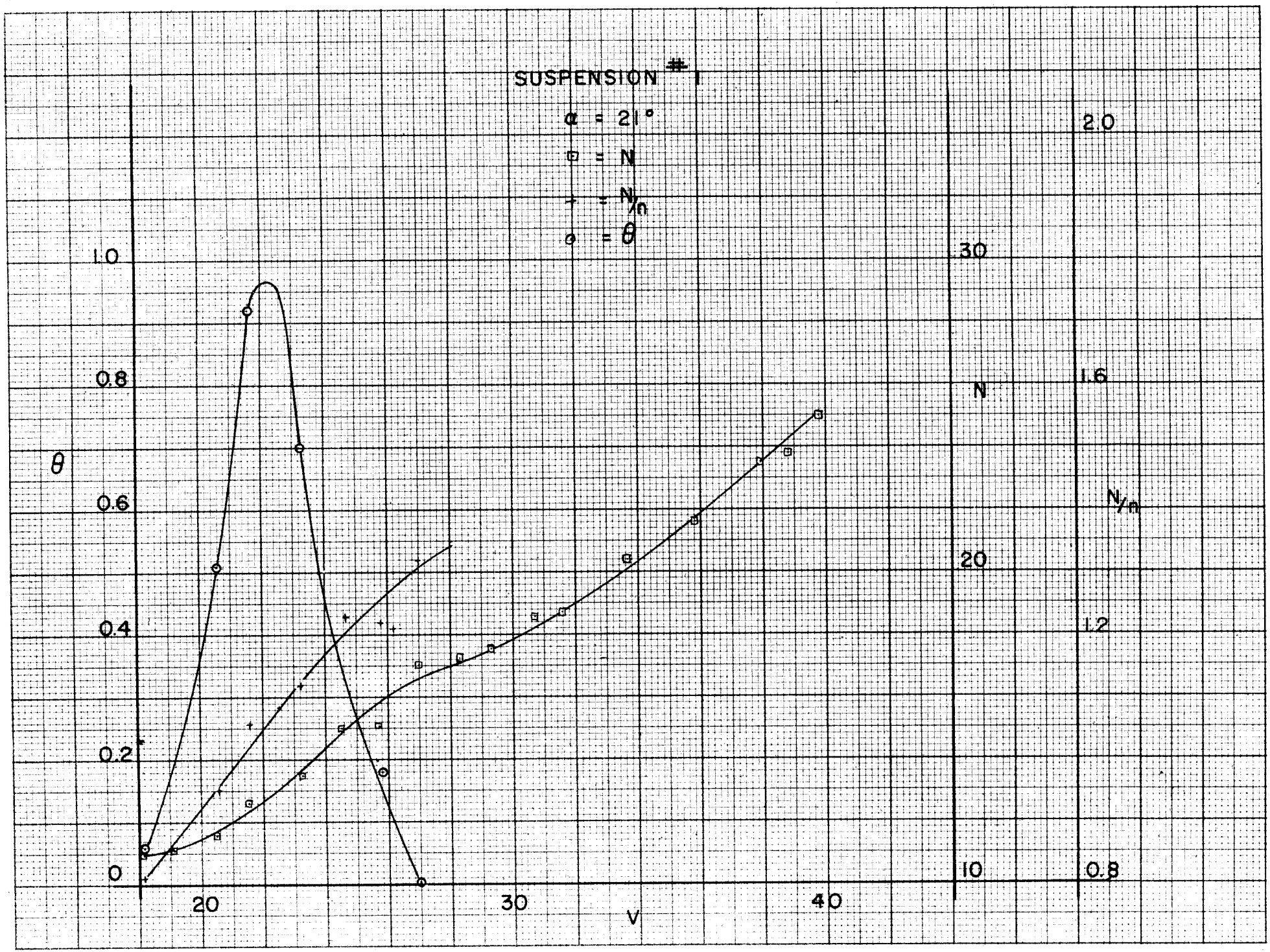
SUSPENSION #1
α = 21°
□ = N
+ = N/n
○ = θ
θ
1.0
0.8
0.6
0.4
0.2
0
20
30
40
V
N
30
20
10
2.0
1.6
1.2
0.8
N/n

FIG. 16

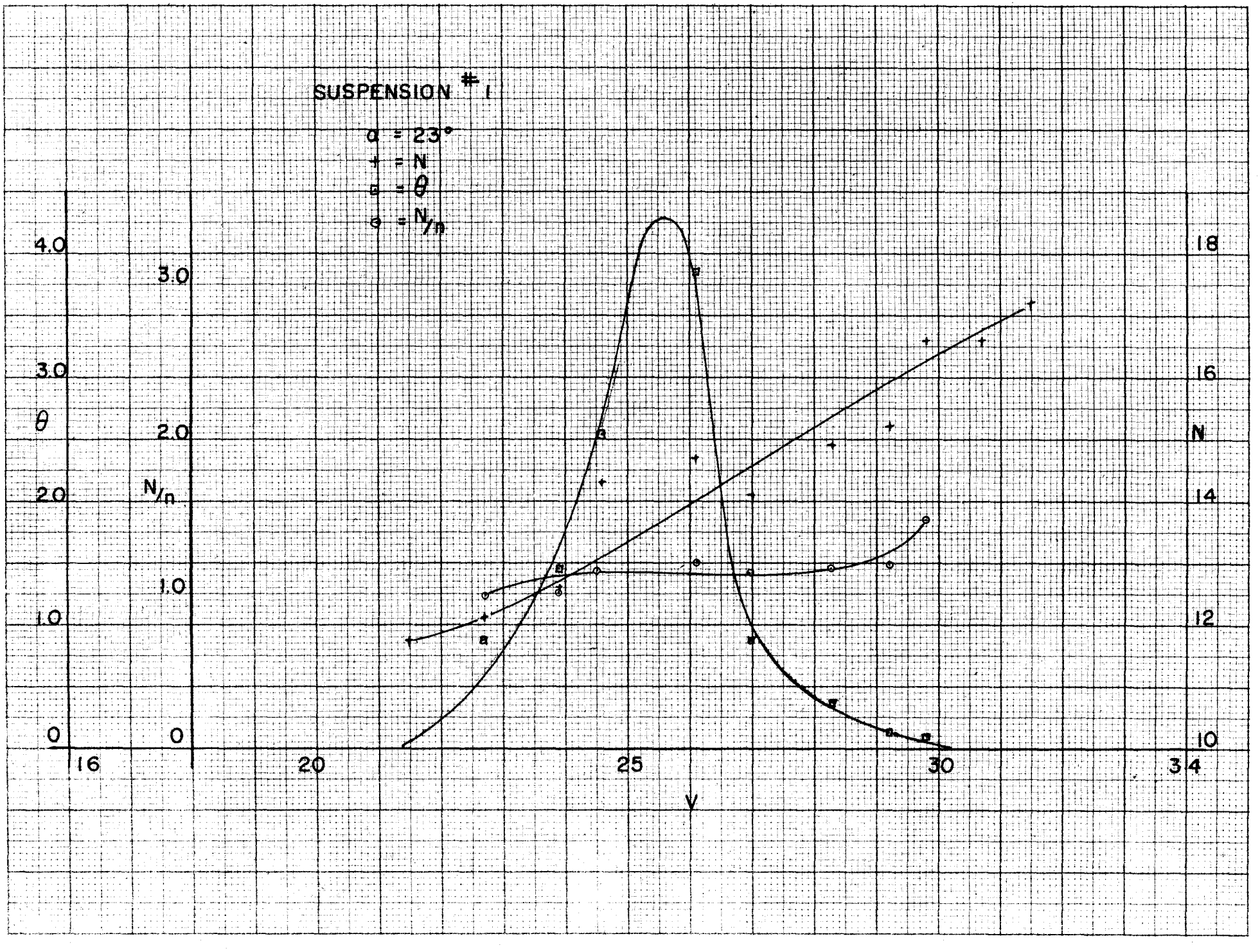
SUSPENSION # 1
α = 23°
+ = N
□ = θ
○ = N/n
4.0
3.0
2.0
1.0
0
θ
N/n
0
16
20
25
30
34
V
18
16
14
12
10
N

FIG. 17

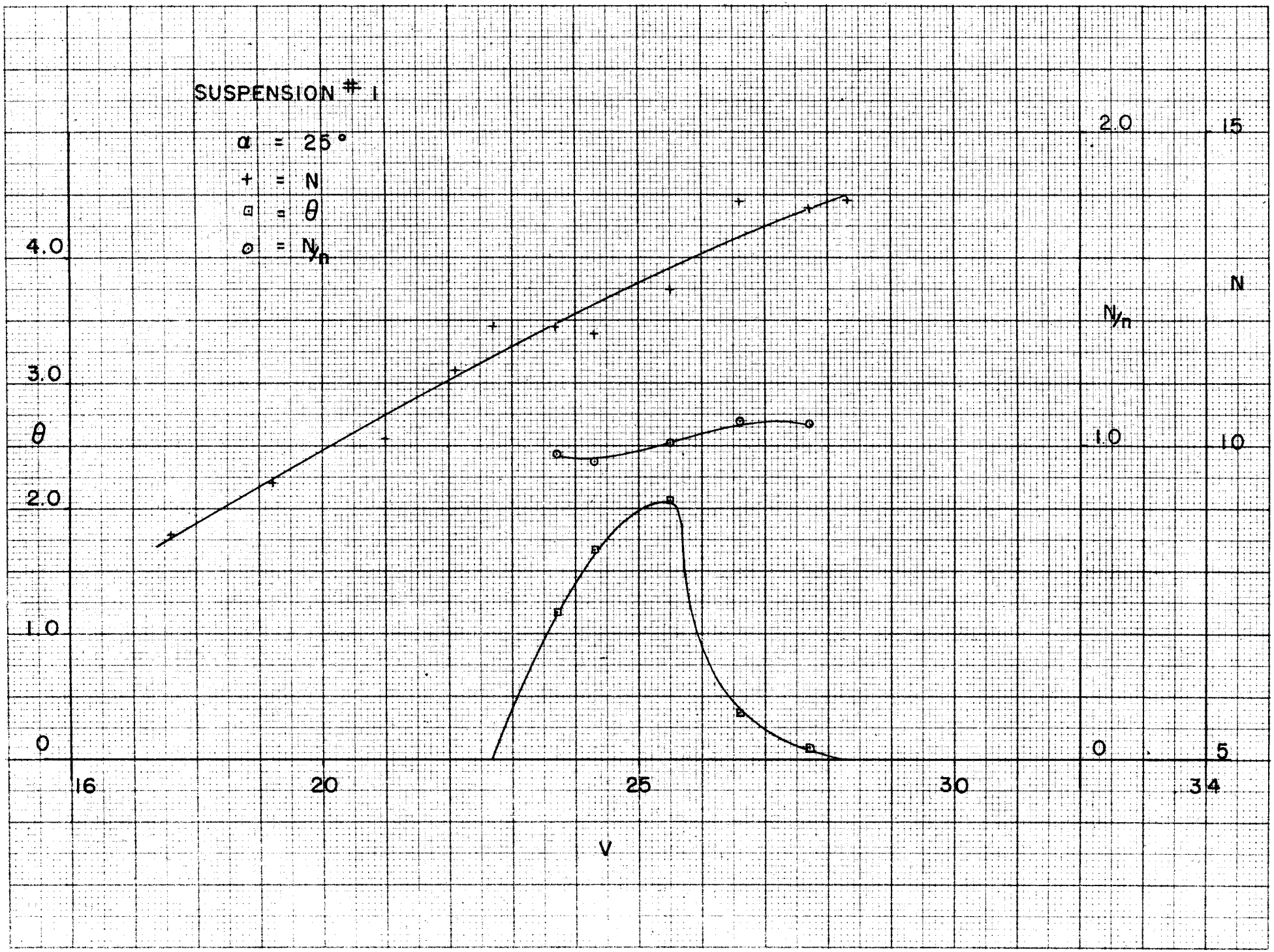
SUSPENSION # 1
α = 25°
+ = N
□ = θ
⊙ = N/n
4.0
3.0
2.0
1.0
0
θ
2.0
1.0
0
N/n
15
10
5
N
16
20
25
30
34
V

FIG. 18

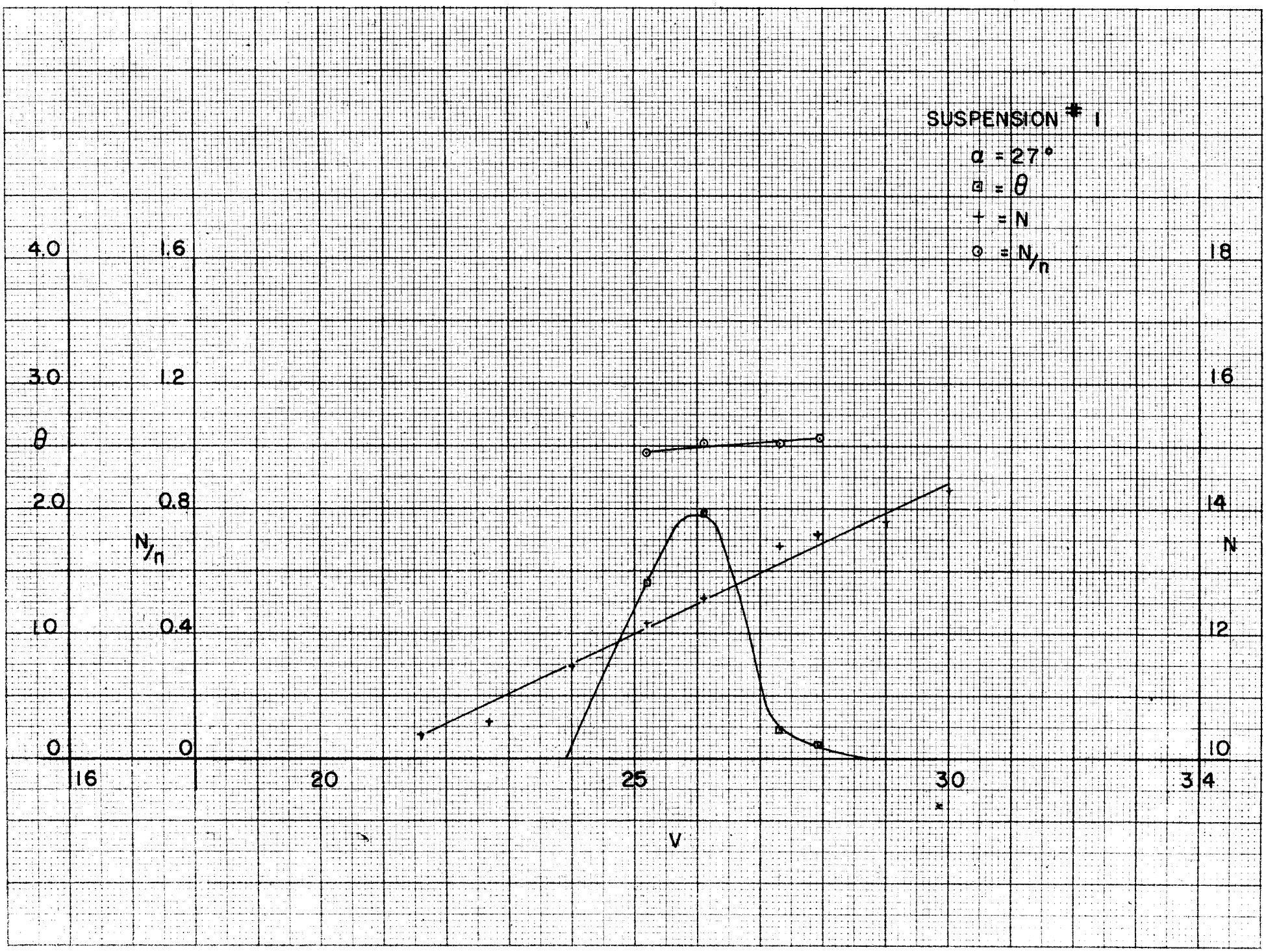
SUSPENSION # 1
α = 27°
□ = θ
+ = N
○ = N/n
4.0
3.0
θ
2.0
1.0
0
1.6
1.2
0.8
N/n
0.4
0
18
16
14
N
12
10
16
20
25
30
34
V

FIG. 19

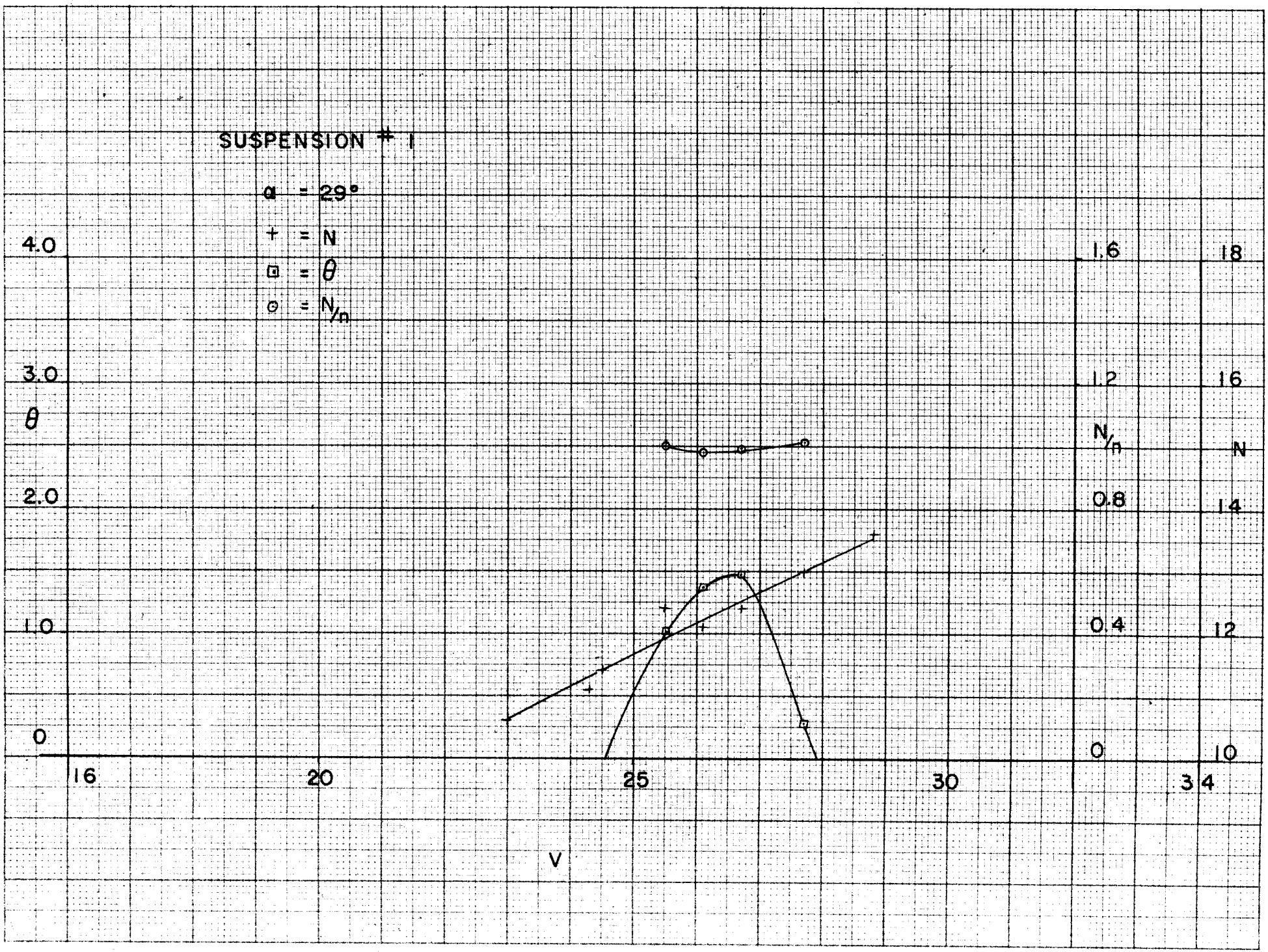
SUSPENSION # 1
α = 29°
+ = N
⊡ = θ
⊙ = N/n
4.0
3.0
θ
2.0
1.0
0
1.6
1.2
N/n
0.8
0.4
0
18
16
N
14
12
10
16
20
25
30
34
V

FIG. 20

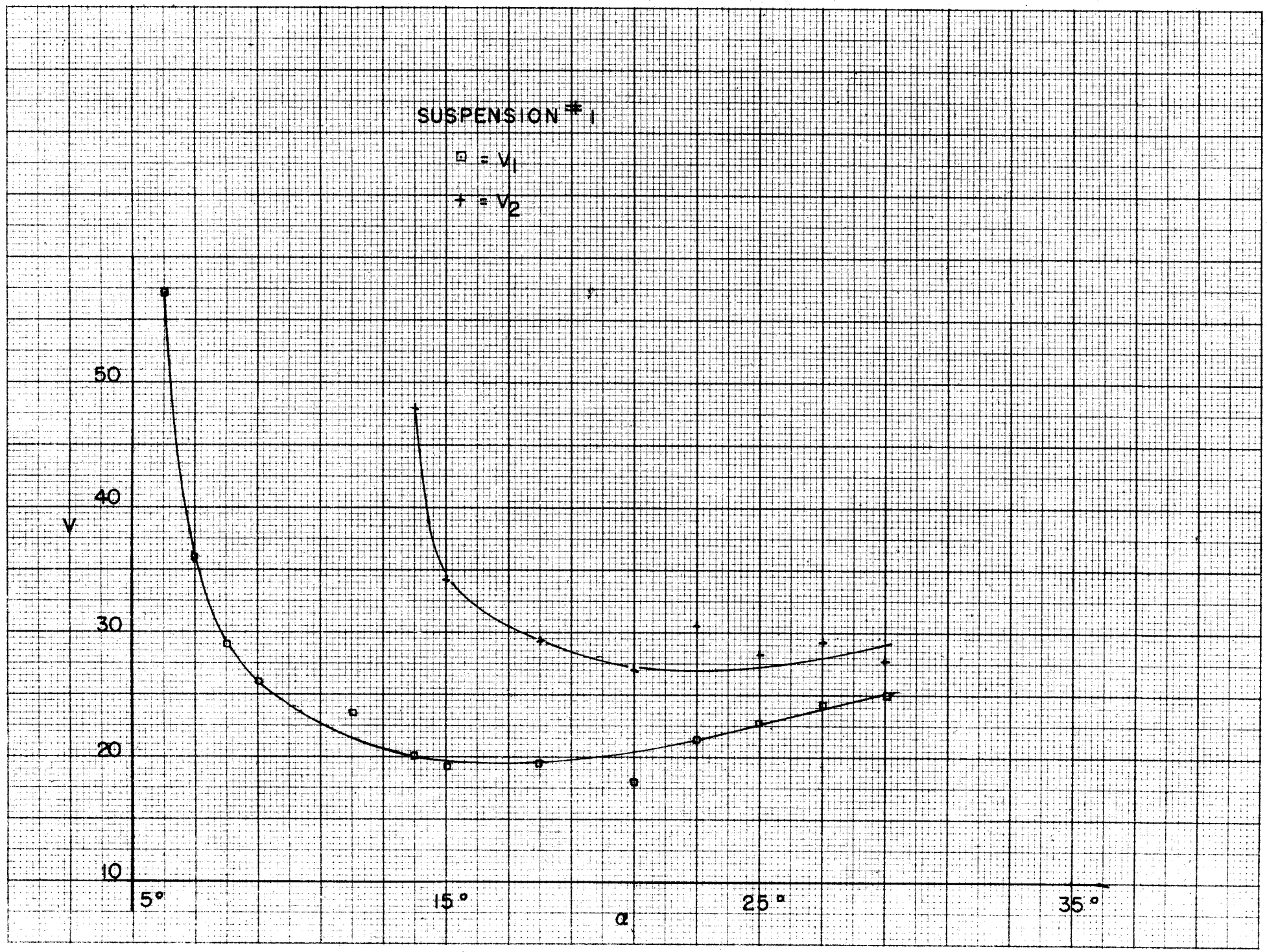

FIG. 21

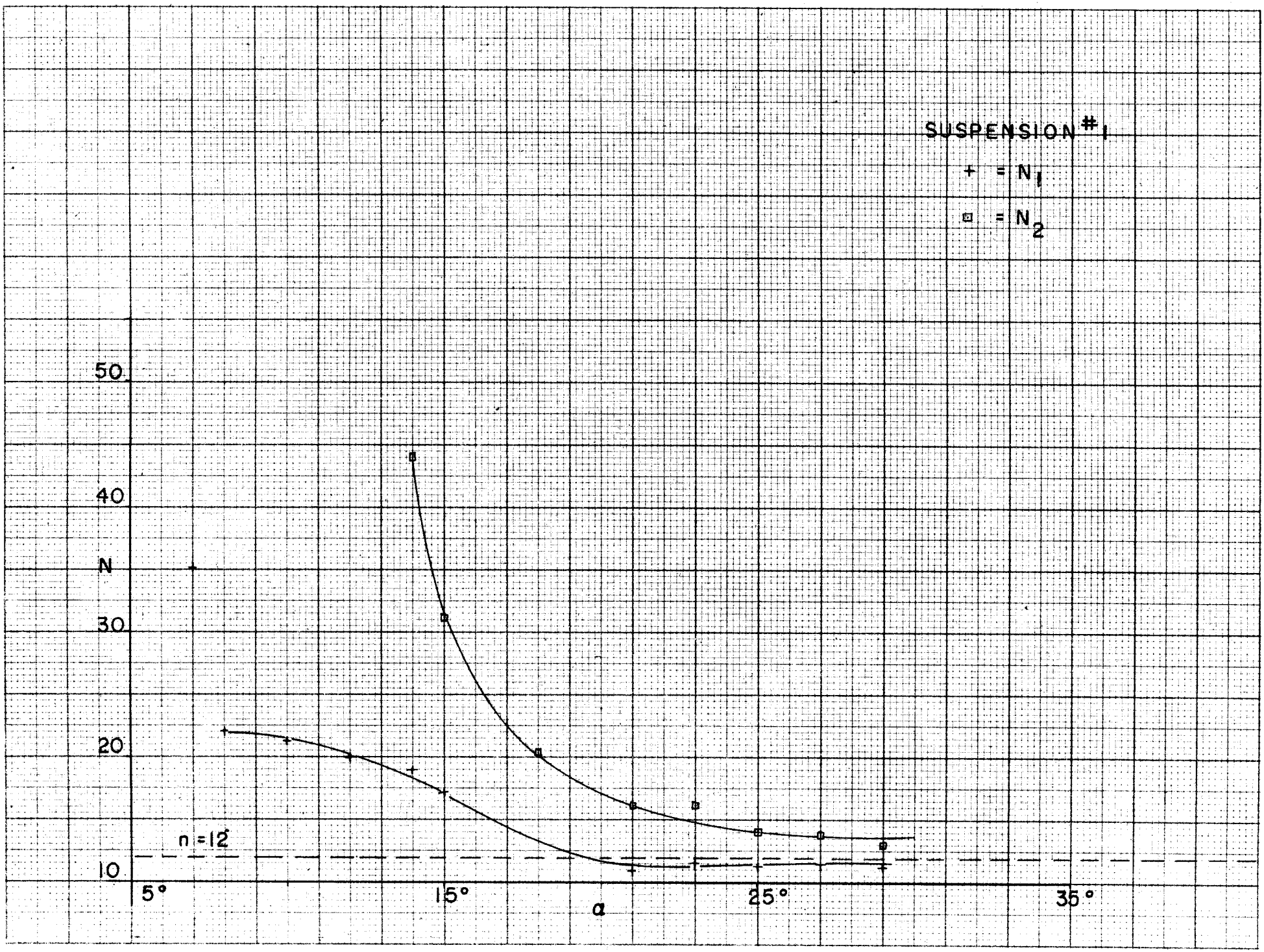

FIG. 22

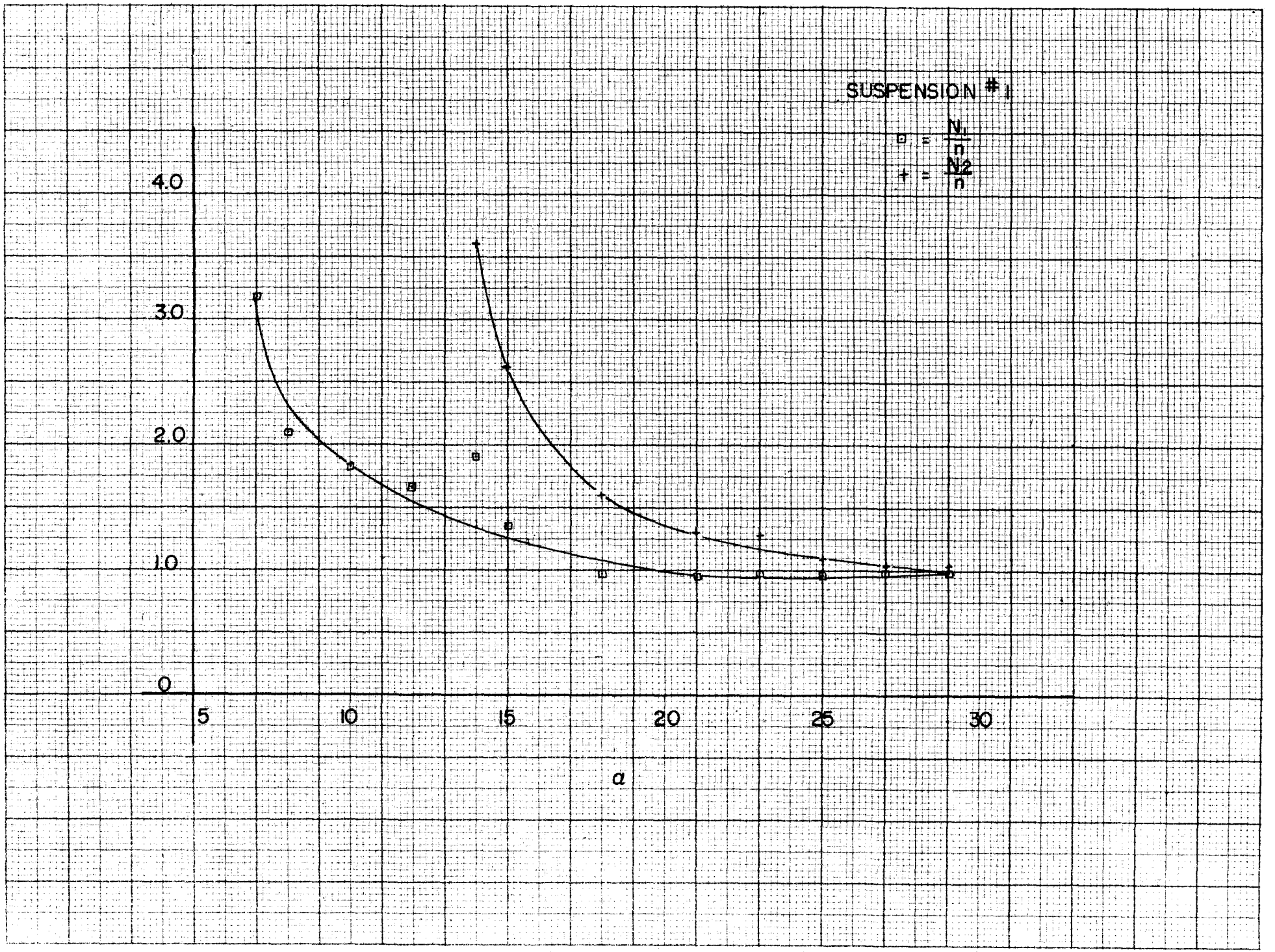

FIG. 23

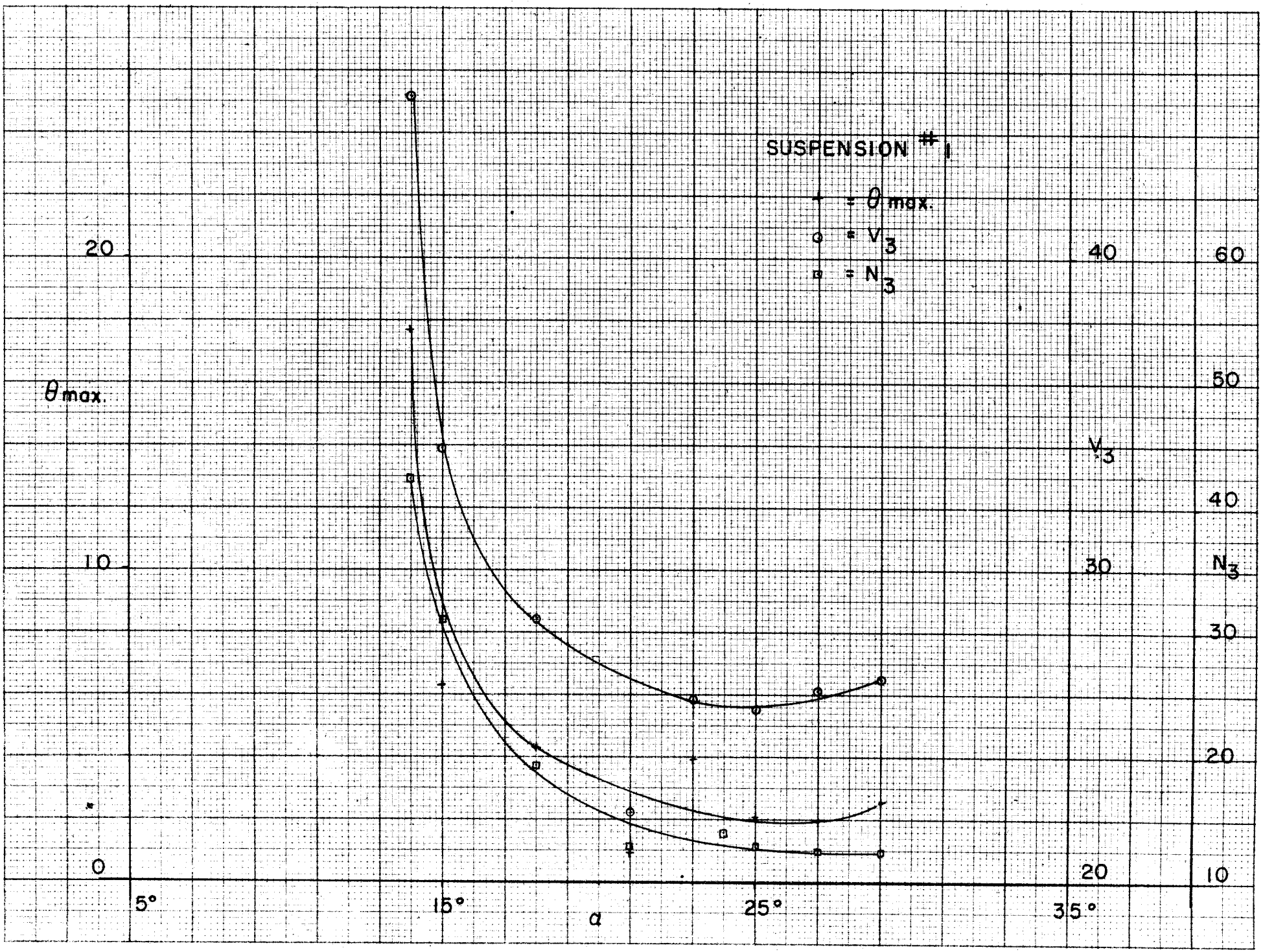
SUSPENSION # 1
+ = θ max.
○ = V3
□ = N3
θ max.
V3
N3
20
10
0
40
30
20
60
50
40
30
20
10
5°
15°
25°
35°
α

FIG. 24

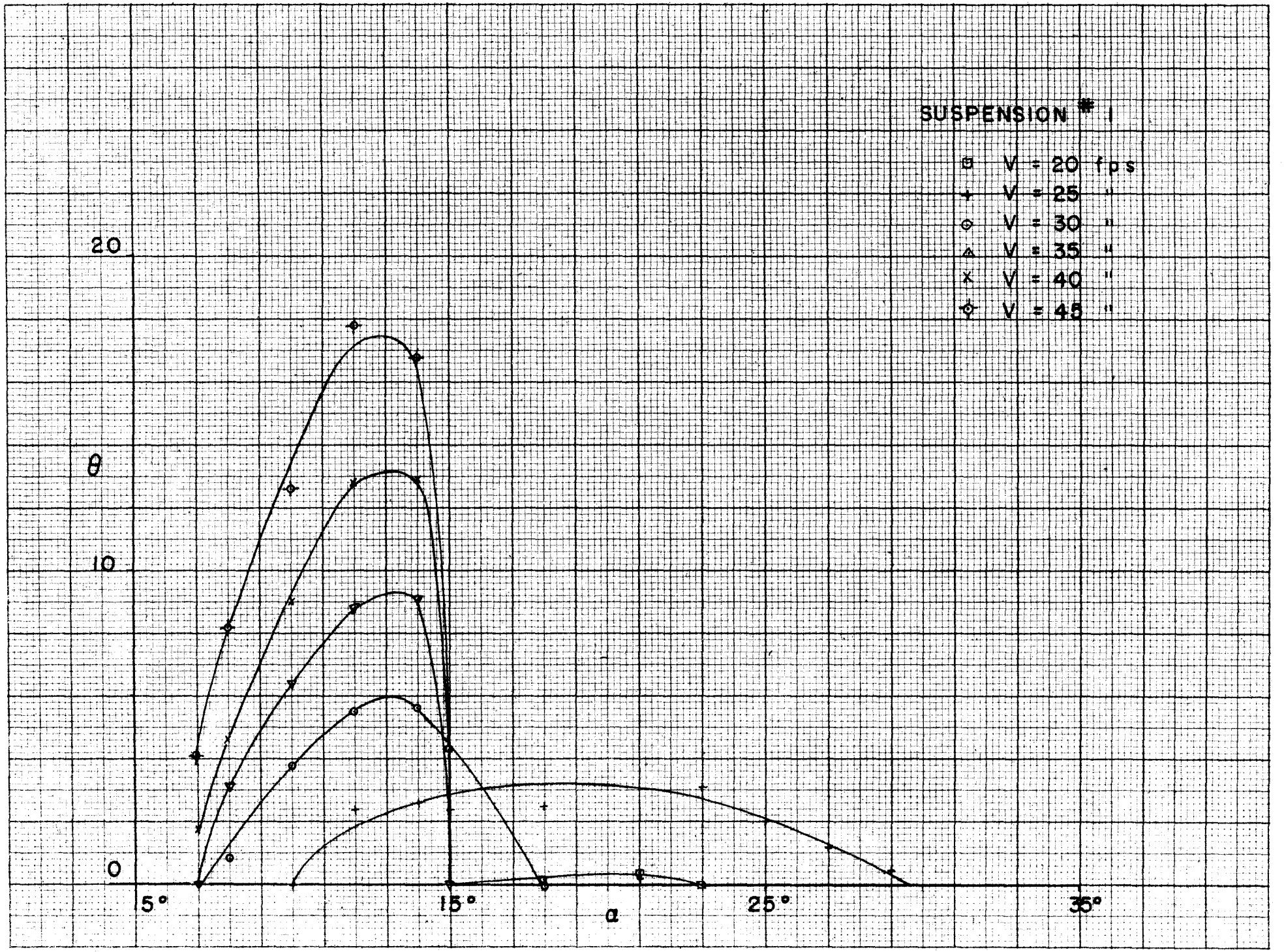

FIG. 25

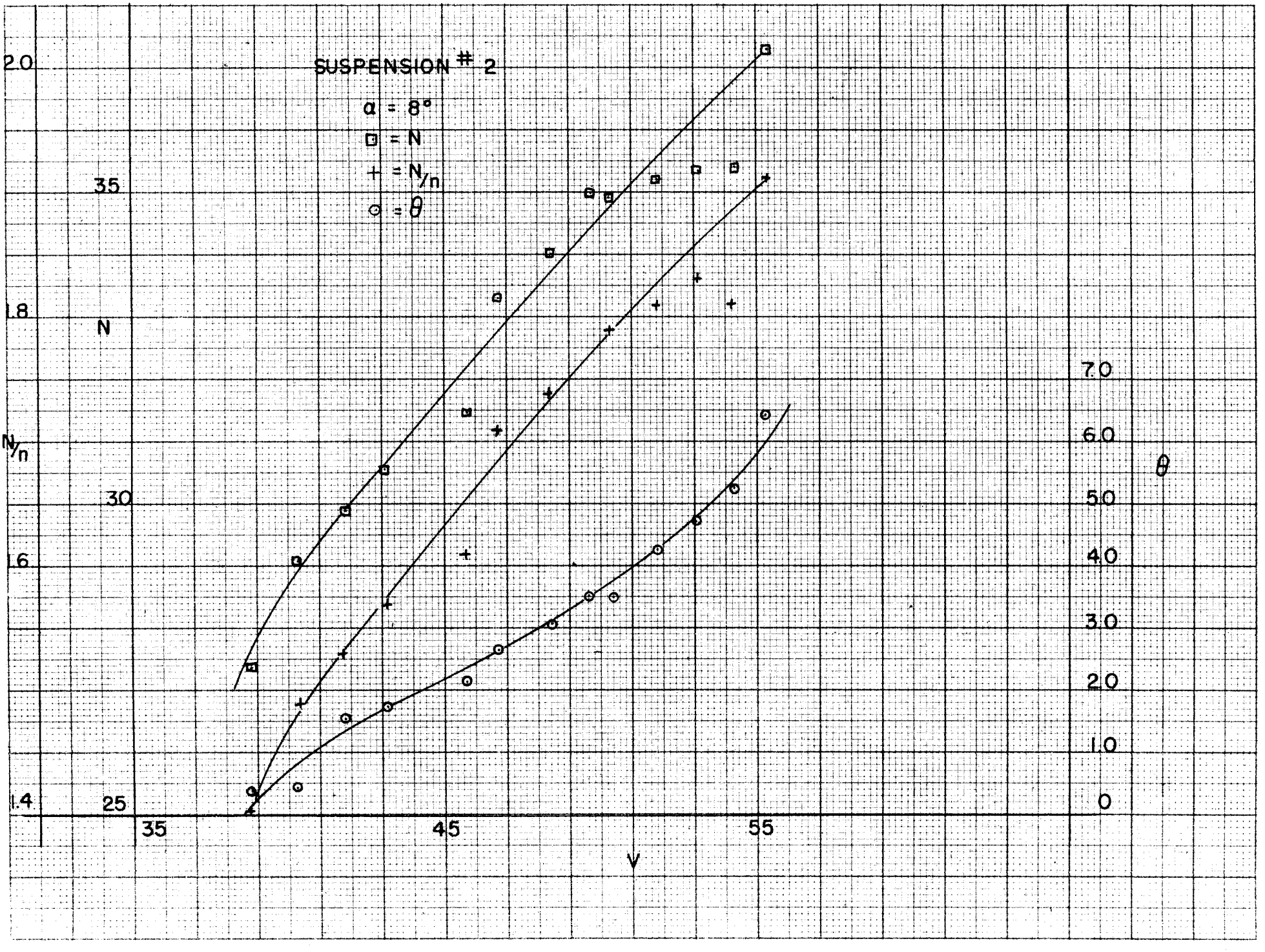
SUSPENSION # 2
α = 8°
□ = N
+ = N/n
⊙ = θ
2.0
1.8
1.6
1.4
N
N/n
35
30
25
7.0
6.0
5.0
4.0
3.0
2.0
1.0
0
θ
35
45
55
V

FIG. 26

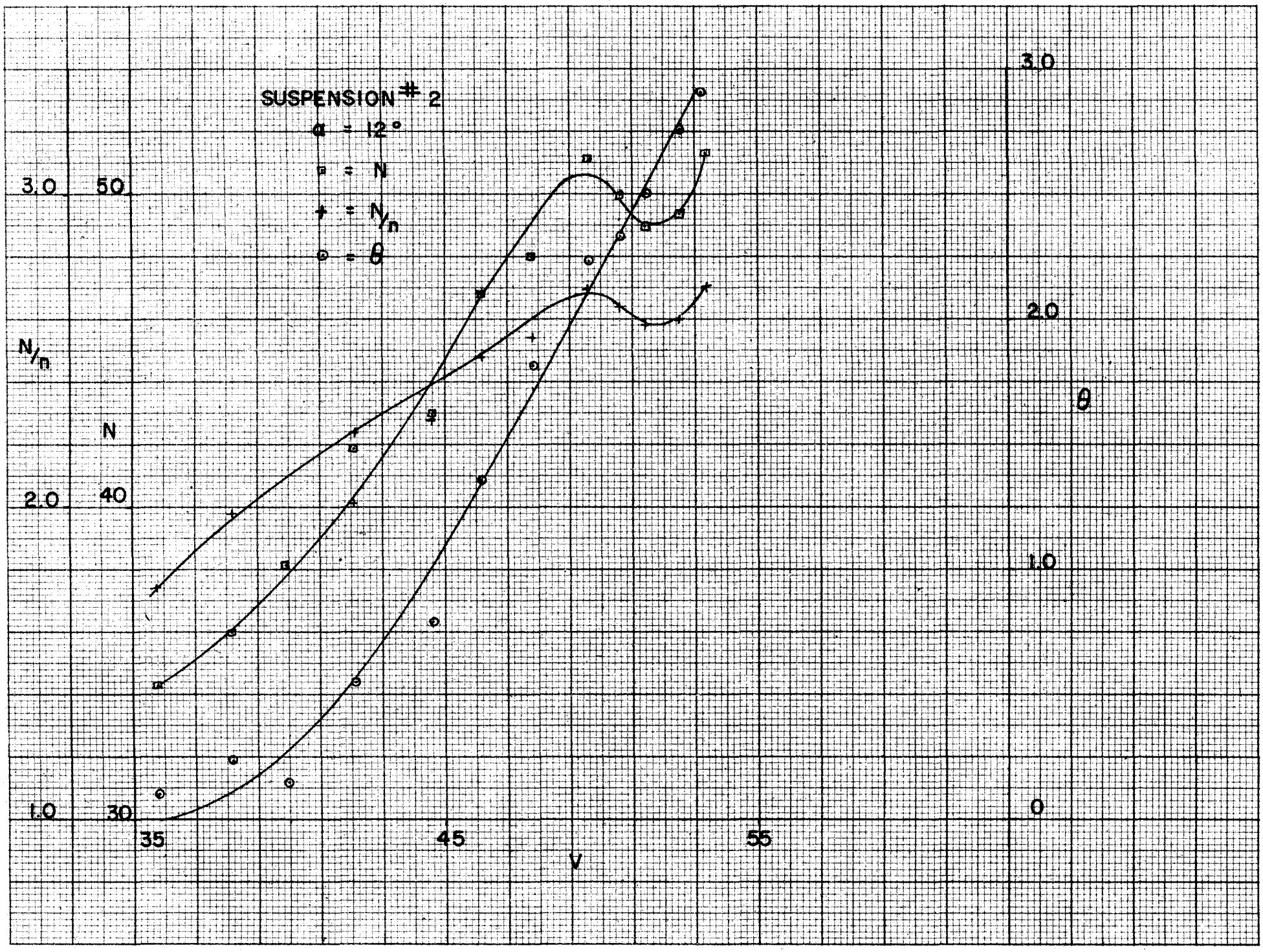

FIG. 27

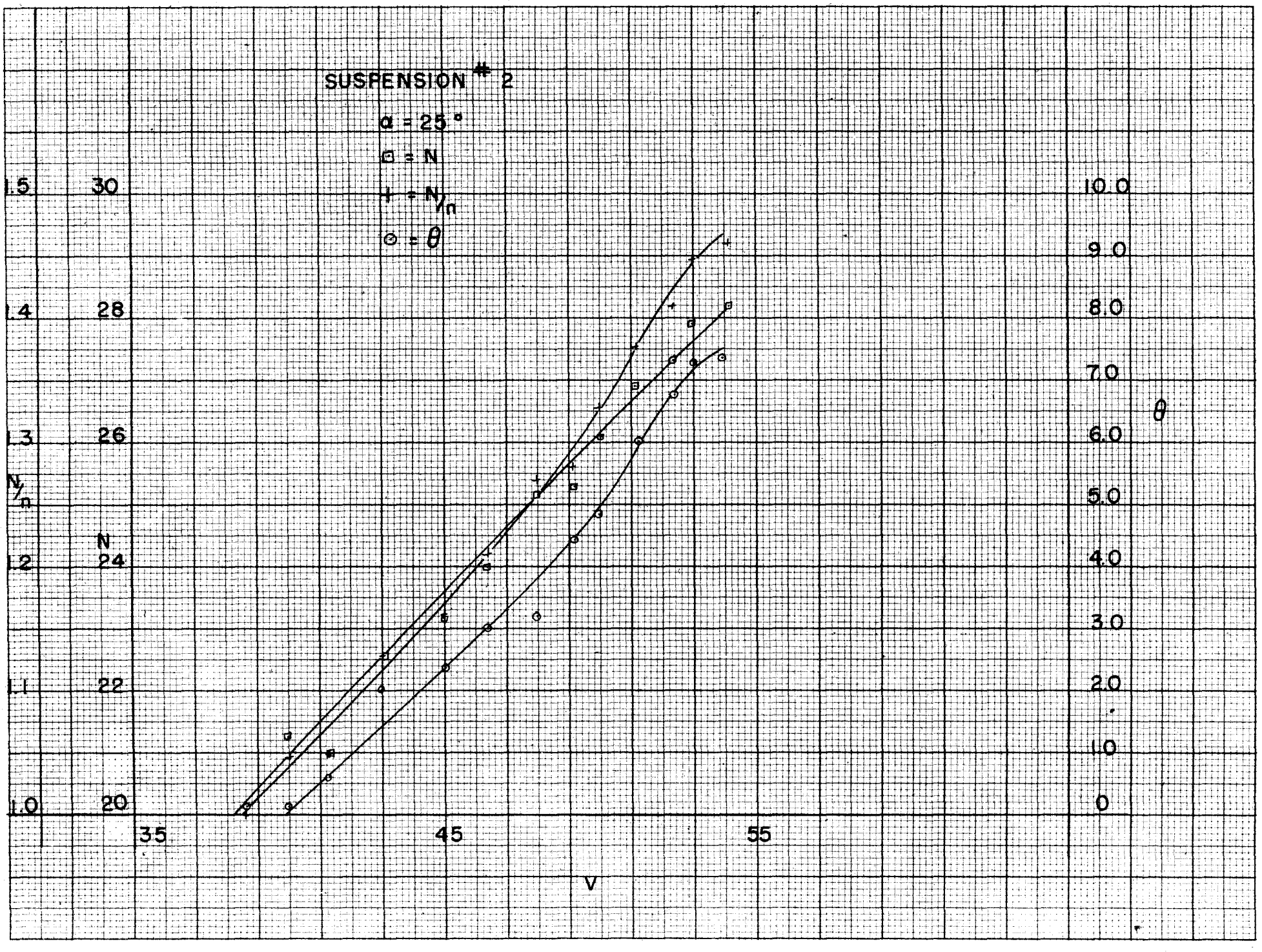
SUSPENSION # 2
α = 25°
□ = N
+ = N/n
⊙ = θ
1.5
1.4
1.3
1.2
1.1
1.0
N/n
30
28
26
24
22
20
N
35
45
55
V
10.0
9.0
8.0
7.0
6.0
5.0
4.0
3.0
2.0
1.0
0
θ

FIG. 28

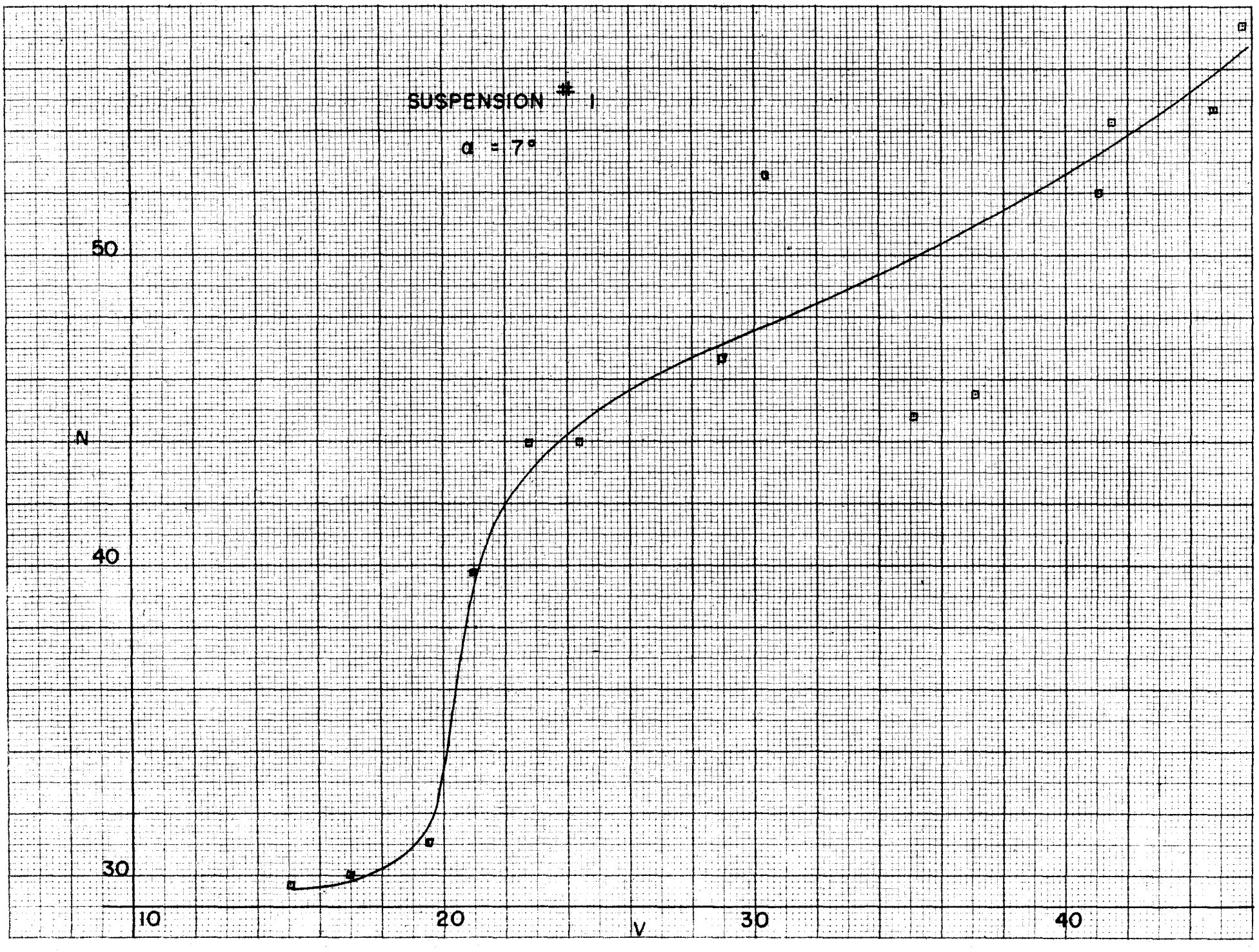

FIG. 29

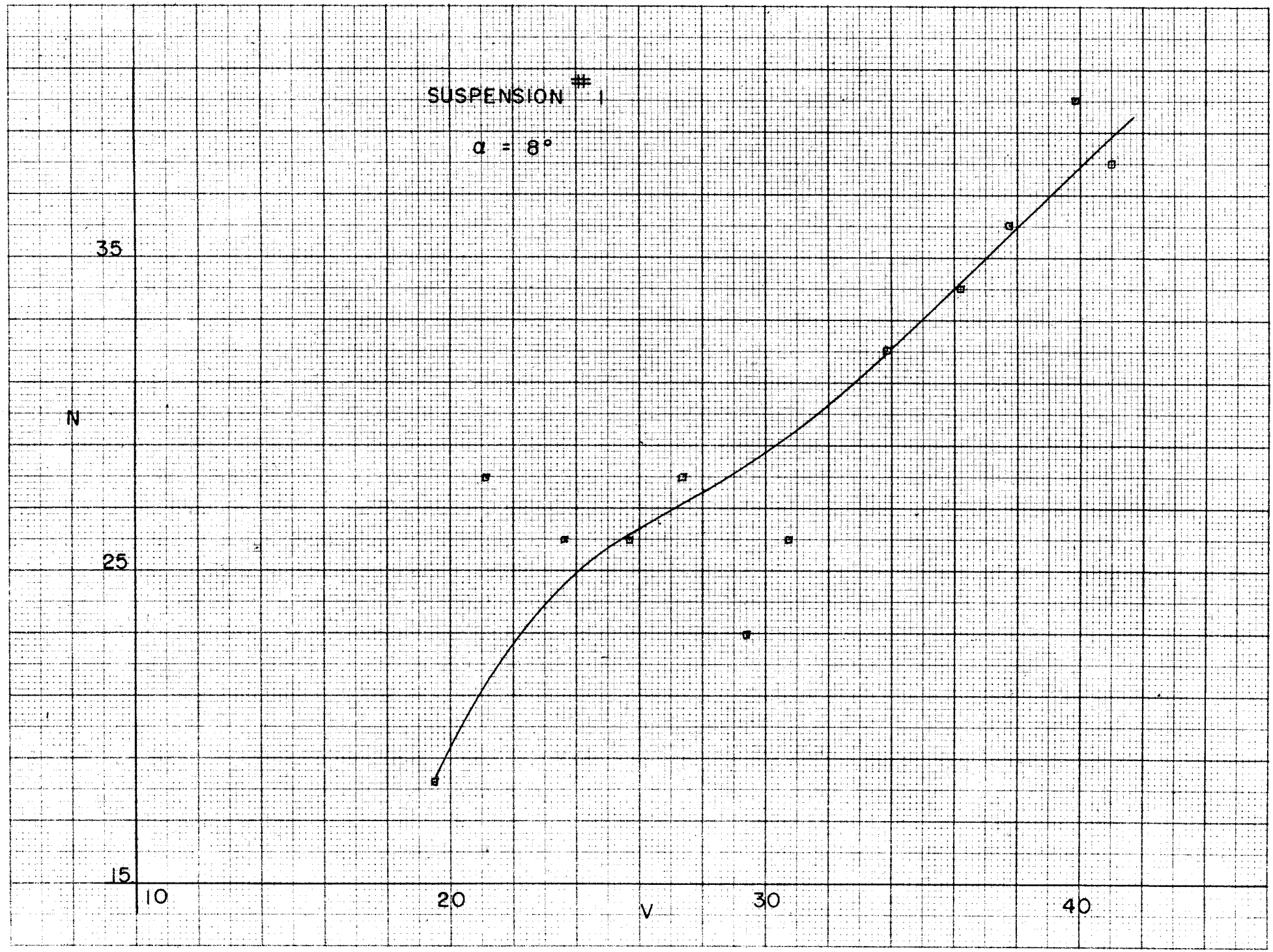

FIG. 30

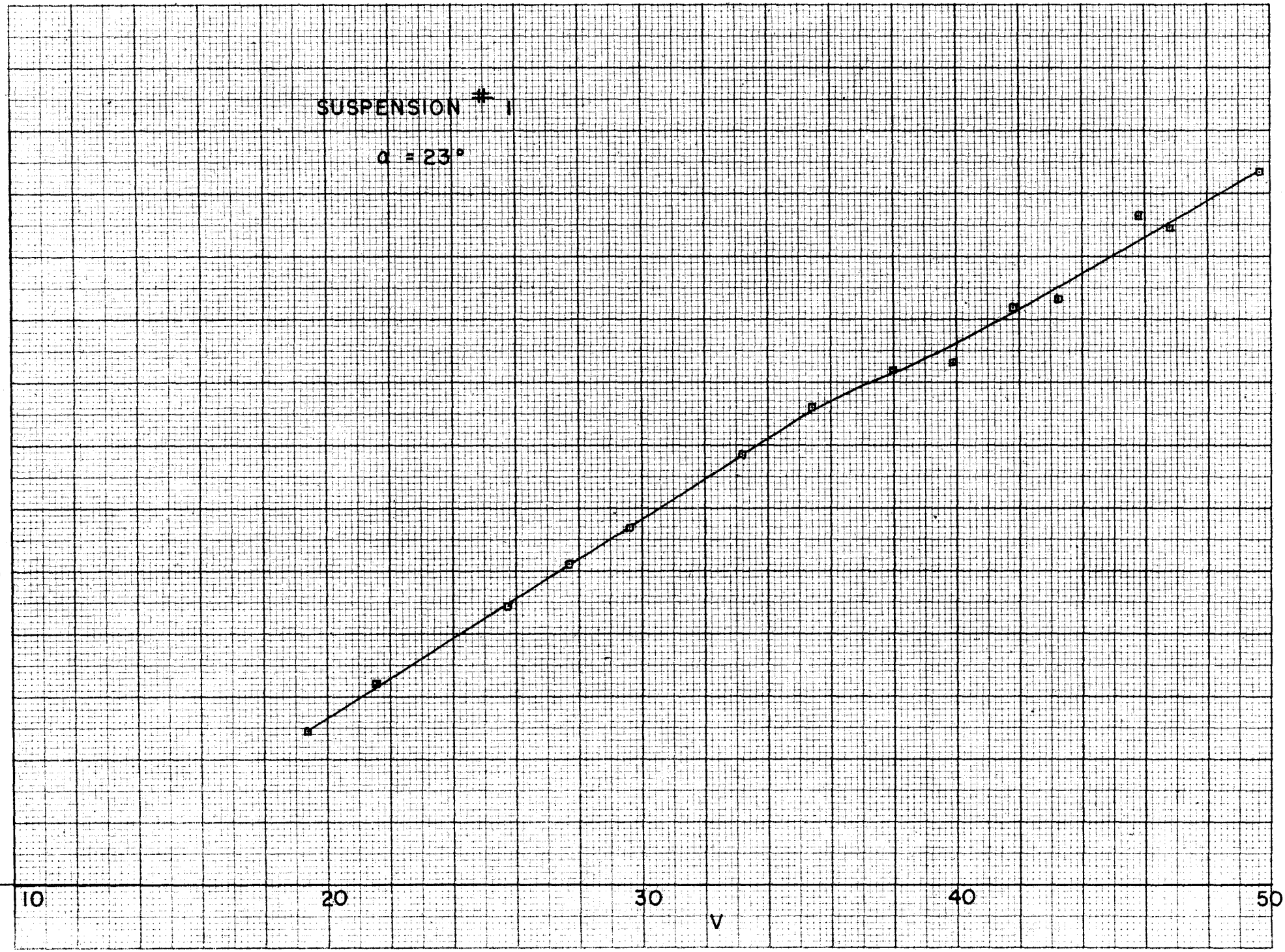

FIG. 31

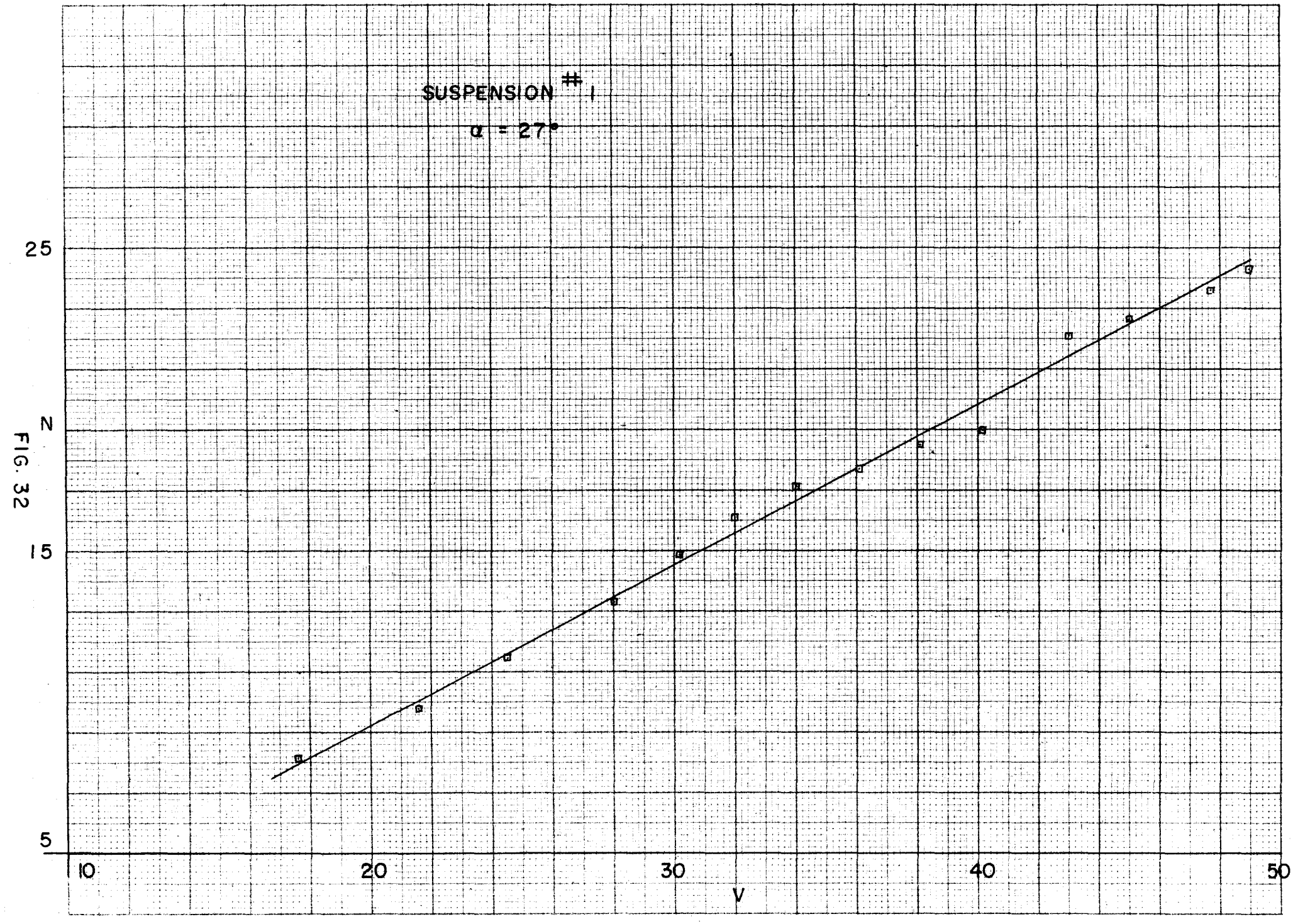

FIG. 32

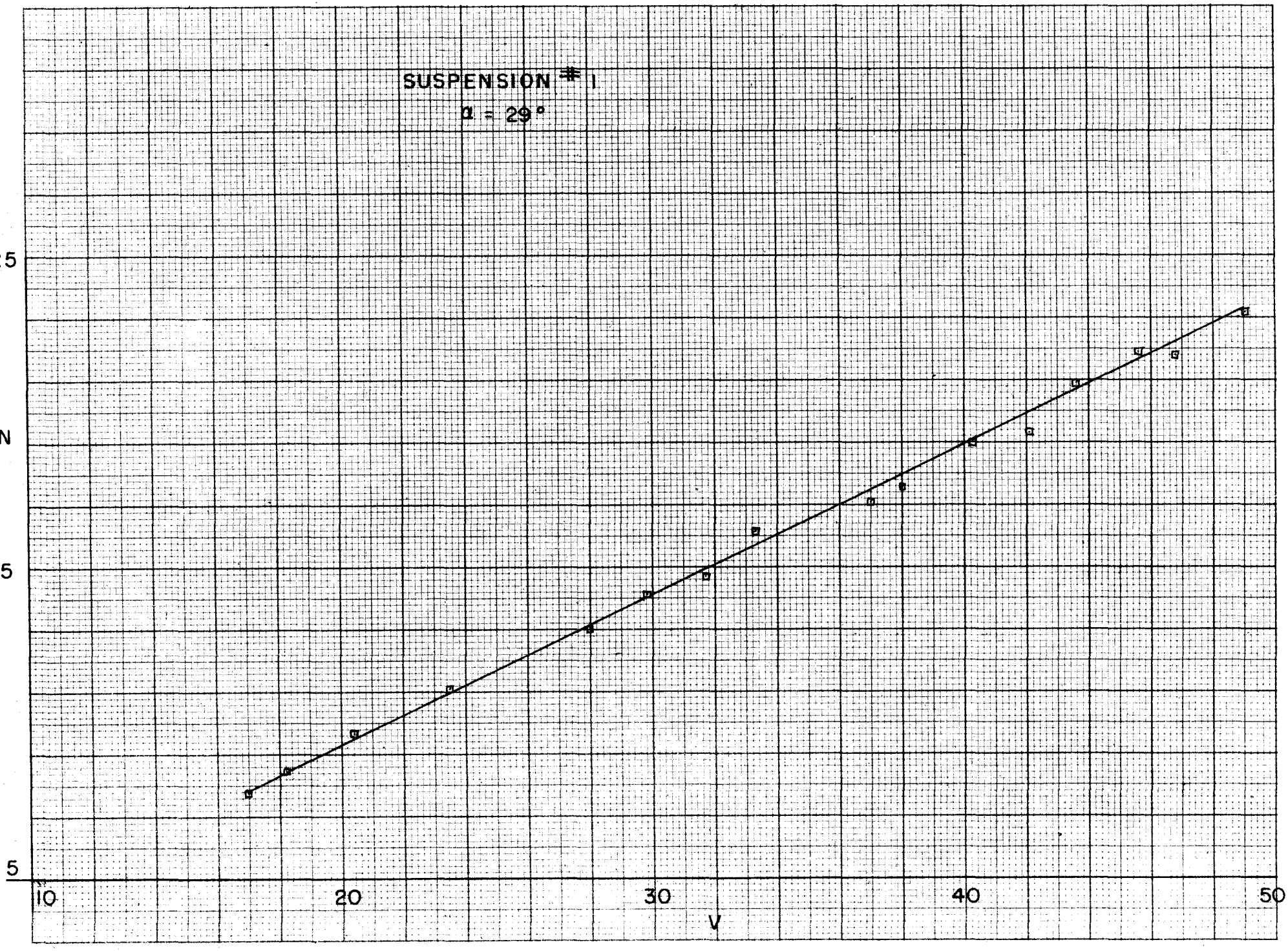

FIG. 33

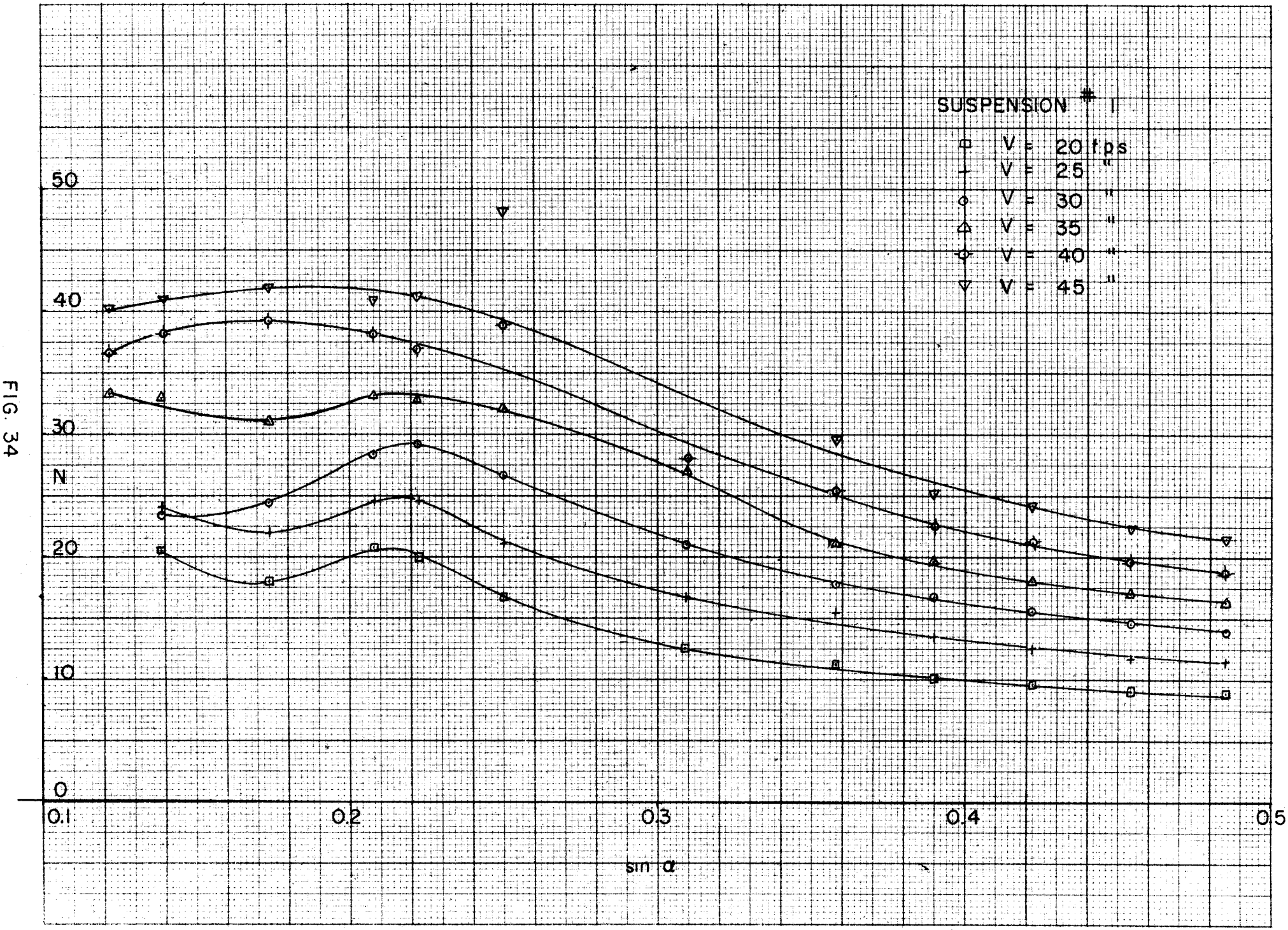
SUSPENSION # 1
V = 20 fps
V = 25 "
V = 30 "
V = 35 "
V = 40 "
V = 45 "
50
40
30
N
20
10
0
0.1
0.2
0.3
0.4
0.5
sin α

FIG. 34

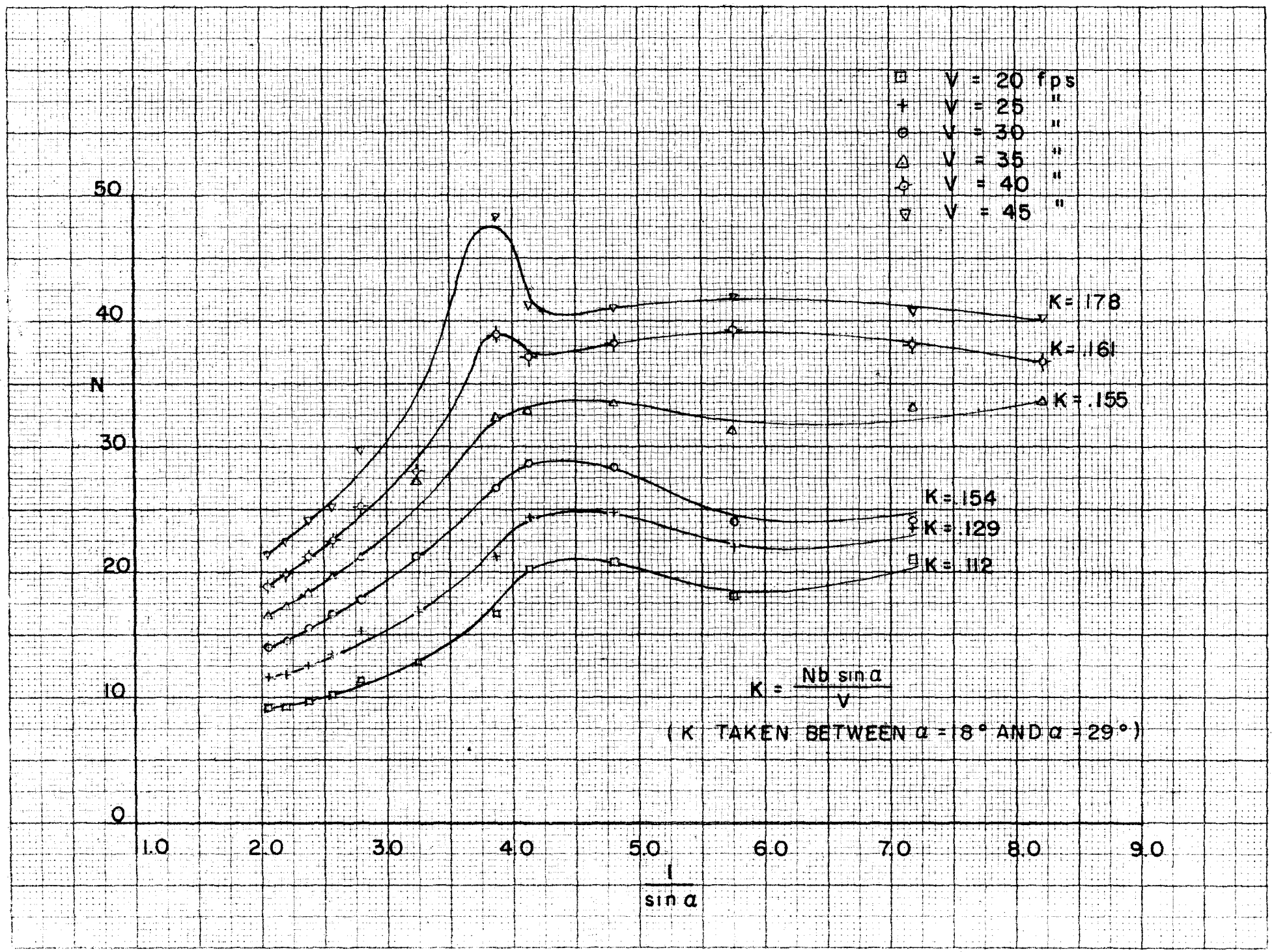
V = 20 fps
V = 25 "
V = 30 "
V = 35 "
V = 40 "
V = 45 "
K = .178
K = .161
K = .155
K = .154
K = .129
K = .112
N
50
40
30
20
10
0
1.0
2.0
3.0
4.0
5.0
6.0
7.0
8.0
9.0
1/sin α
K = Nb sin α / V
(K TAKEN BETWEEN α = 18° AND α = 29°)

FIG. 35

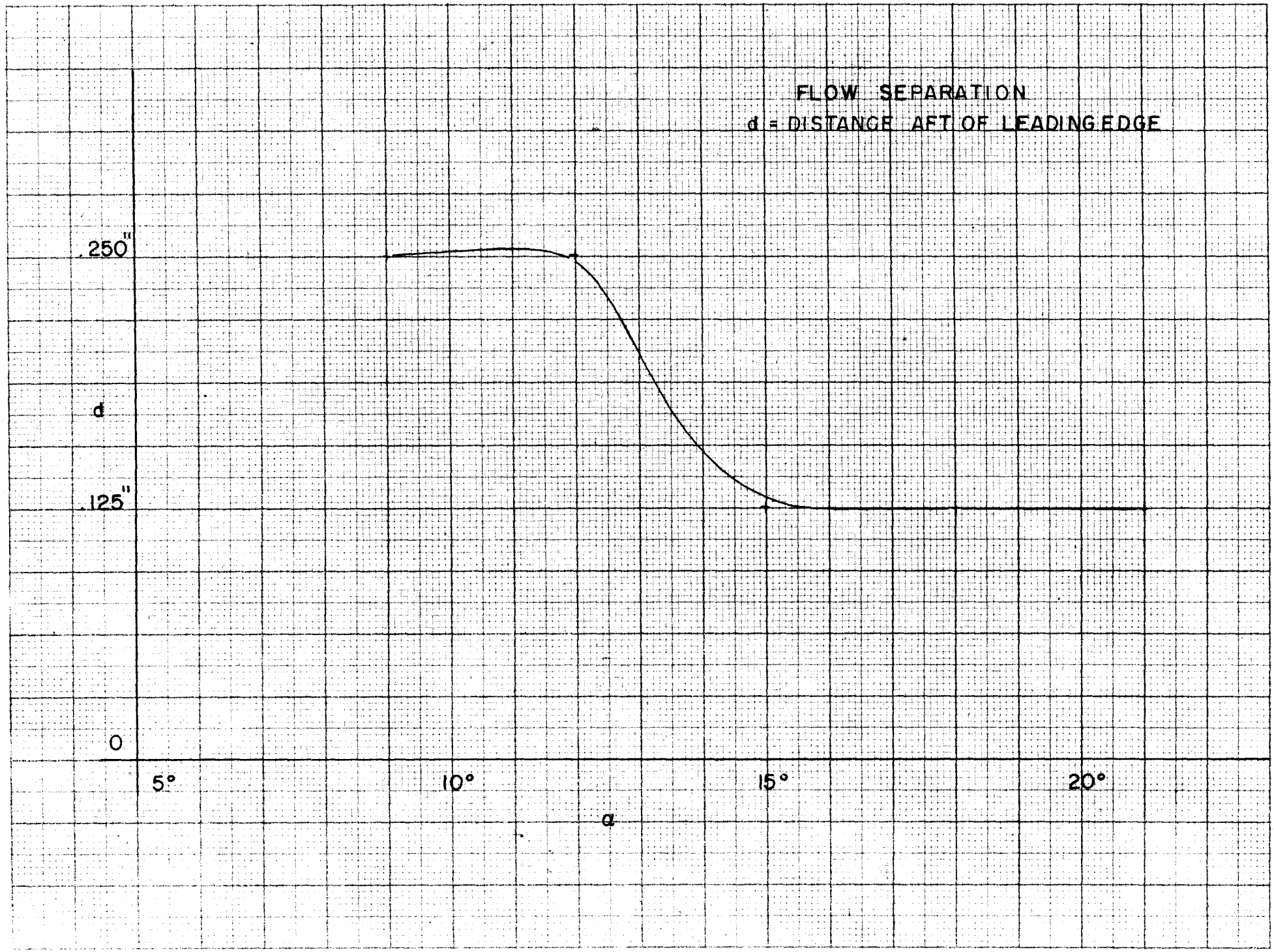
FLOW SEPARATION
d = DISTANCE AFT OF LEADING EDGE
.250"
d
.125"
0
5°
10°
15°
20°
α

FIG. 36

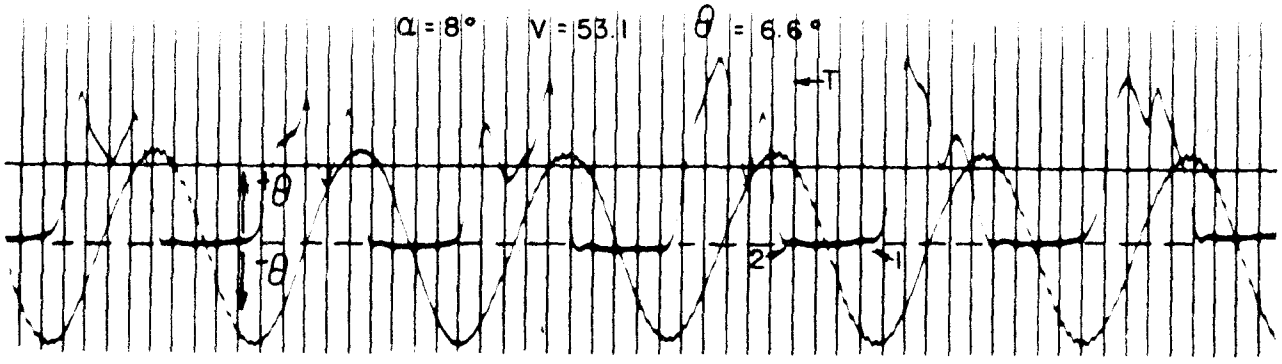
α = 8°
V = 53.1
θ = 6.6°
T
θ
-θ
2
1

a

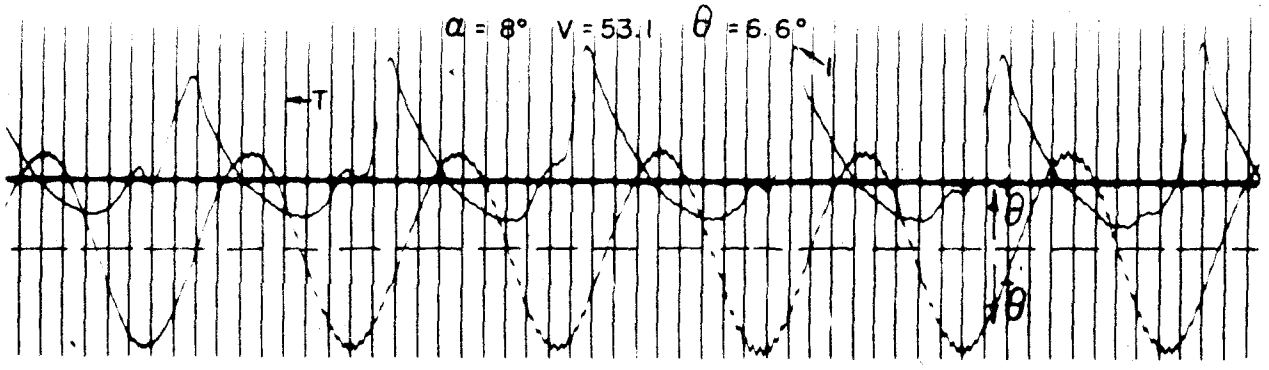
α = 8°
V = 53.1
θ = 6.6°
1
T
θ
-θ

b

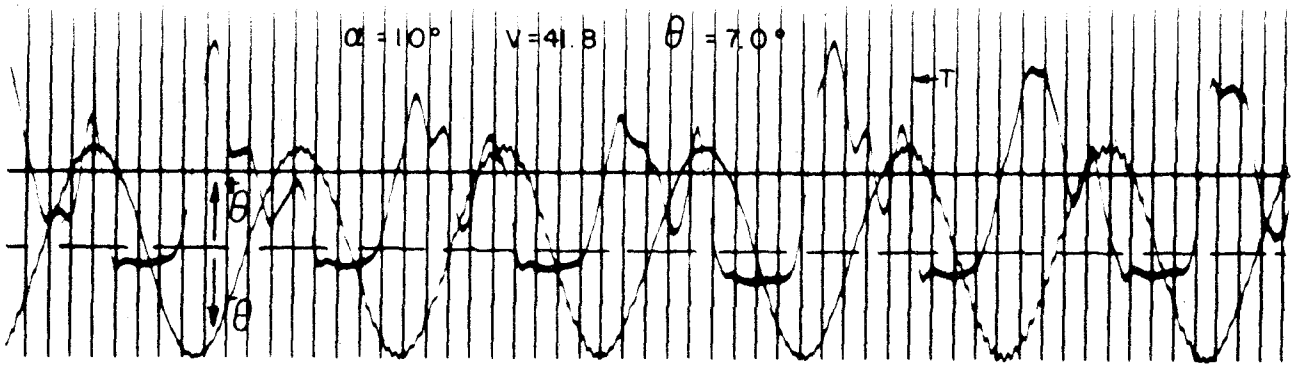
α = 10°
V = 41.8
θ = 7.0°
T
θ
-θ

c

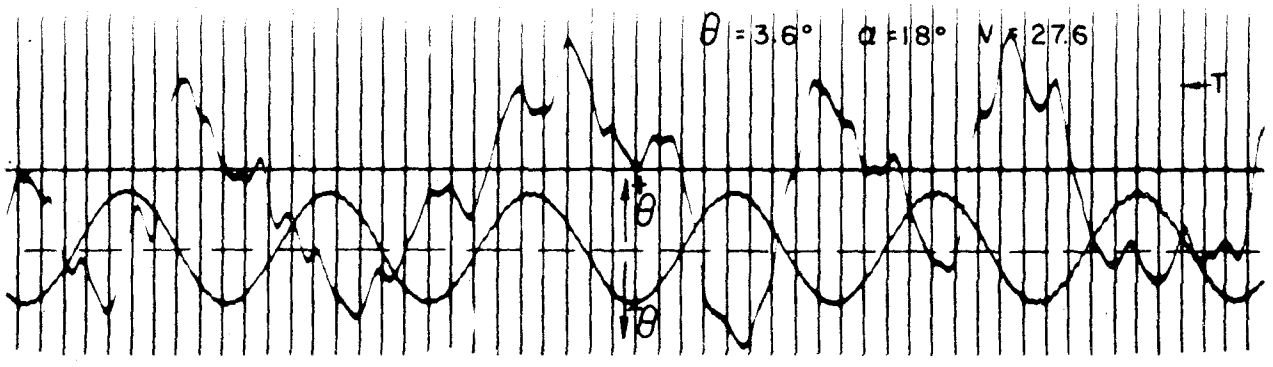
θ = 3.6°
α = 18°
V = 27.6
T
θ
-θ

d

FIG. 37